Tension dynamics in semiflexible polymers. II. Scaling solutions and applications

Oskar Hallatschek,[1,*] Erwin Frey,[2] and Klaus Kroy[3]
[1]*Lyman Laboratory of Physics, Harvard University, Cambridge, Massachusetts 02138, USA*
[2]*Arnold Sommerfeld Center for Theoretical Physics and Center for NanoScience, LMU München, Theresienstrasse 37, 800333 München, Germany*
[3]*Institut für Theoretische Physik, Universität Leipzig, Augustusplatz 10/11, 04109 Leipzig, Germany*
(Received 27 September 2006; published 7 March 2007)

In part I [O. Hallatschek *et al.*, preceding paper, Phys. Rev. E **75**, 031905 (2007)] of this contribution, a systematic coarse-grained description of the dynamics of a weakly bending semiflexible polymer was developed. Here, we discuss analytical solutions of the established deterministic partial integro-differential equation for the spatiotemporal relaxation of the backbone tension. For prototypal experimental situations, such as the sudden application or release of a strong external pulling force, it is demonstrated that the tensile dynamics reflects the self-affine conformational fluctuation spectrum in a variety of intermediate asymptotic power laws. Detailed and explicit analytical predictions for the tension propagation and relaxation and corresponding results for common observables, such as the end-to-end distance, are obtained.

DOI: 10.1103/PhysRevE.75.031906 PACS number(s): 87.15.He, 87.15.Aa, 87.16.Ka, 83.10.−y

I. INTRODUCTION

Polymer physics has traditionally focused on very flexible polymers that admit a highly coarse-grained description in terms of Gaussian chains and exhibit universal physical behavior that can be explained using methods from statistical mechanics such as the renormalization group and scaling arguments [1]. Further research has explored new terrain that lies beyond the realm of applicability of this highly successful approach either because the polymers of interest are too stiff or because they are subject to extreme forces. Many of these instances have recently appeared in applications involving biopolymers. Notorious examples are the nonlinear mechanical response of DNA [2], which has turned out to be pivotal to protein-DNA interactions, and the problem of force transduction through the cytoskeleton [3–5], which is a major mechanism by which cells explore their environment and react to external mechanical stimuli. Clearly, in neither of these situations can theorists contend themselves with the convenient Gaussian chain representation, but have to resort to more realistic, yet still schematic descriptions, such as the freely-jointed chain (e.g., for single-stranded DNA) or the wormlike chain model (for double-stranded DNA, F-actin, microtubules, etc.) [1,6].

Suspicions that this might entail a substantial loss of universality and render systematic analytical approaches forbiddingly complex have turned out to be unfounded. The wormlike chain model provides an analytically tractable standard model for many of the above-mentioned new applications, in particular for calculating the nonequilibrium dynamical response of stiff and semiflexible but weakly bending polymers to strong external fields. As established in part I [7] of this contribution, the weakly bending wormlike chain lends itself to a multiple-scale perturbation theory (MSPT) based on a length scale separation between longitudinal and transverse dynamic correlation lengths. In the present part II, we demonstrate that the self-affine roughness, acquired by the weakly bending contour in thermal equilibrium, plays an analogous role as the more familiar fractal conformational correlations in the case of flexible polymers [1]. The self-similarity of the static conformational fluctuations entails self-similar dynamics. It manifests itself in a variety of *intermediate asymptotic dynamic power laws*. Apart from the restriction to polymers with a (locally) rodlike structure, these predictions are as universal as those of classical polymer physics. They are, moreover, derived in a direct way, usually including exact amplitudes, from a controlled perturbation expansion.

As a major result of the multiple-scale theory developed in part I, we obtained a coarse-grained reformulation of the free-draining Langevin equations of motion of a weakly bending rod in the form of the deterministic equation

$$\partial_s^2 F(s,t) = -\zeta_\parallel \langle \Delta\overline{\varrho}\rangle[F(s,\tilde{t}\le t),t]. \tag{1}$$

It describes the long-wavelength (all time) dynamics of the time-integrated tension

$$F(s,t) \equiv \int_0^t dt' f(s,t'), \tag{2}$$

with $\zeta_\parallel$ being the friction coefficient for longitudinal motion and $\langle \Delta\overline{\varrho}\rangle[F(s,\tilde{t}\le t),t]$ the average release of contour length stored in the transverse undulations up to time t. Written out in terms of the transverse normal-mode contributions, the latter reads

$$\langle \Delta\overline{\varrho}\rangle(t) \equiv \int_0^\infty \frac{dq}{\pi\ell_p}\left\{\frac{1}{q^2+f_<}(e^{-2q^2[\kappa q^2 t+F(t)]/\zeta_\perp}-1) + 2q^2\int_0^t d\tilde{t} e^{-2q^2[\kappa q^2(t-\tilde{t})+F(t)-F(\tilde{t})]/\zeta_\perp}\right\}, \tag{3}$$

where κ, $\ell_p=\kappa/(k_BT)$, and $\zeta_\perp$ are the bending stiffness, persistence length, and friction coefficient for transverse motion, respectively. The parameter $f_< \equiv f(t<0)=\text{const}$ allows one

*Electronic address: ohallats@fas.harvard.edu

to take into account a constant pre-stress.[1] Upon inserting this dynamical force-extension relation into Eq. (1), we arrived at our central result, the closed partial integro-differential equation (PIDE) for the time-integrated tension $F(s,t)$,

$$\partial_s^2 F(s,t) = \hat{\zeta}\int_0^\infty \frac{dq}{\pi\ell_p}\left\{\frac{1}{q^2+f_<}(1-e^{-2q^2[q^2t+F(s,t)]}) - 2q^2\int_0^t d\tilde{t}\, e^{-2q^2[q^2(t-\tilde{t})+F(s,t)-F(s,\tilde{t})]}\right\}. \quad (4)$$

For convenience, we have made the following choice of units: Time and tension, respectively, are rescaled according to

$$t \to \zeta_\perp t/\kappa, \quad (5)$$

$$f \to \kappa f. \quad (6)$$

This corresponds to setting $\kappa \equiv \zeta_\perp \equiv 1$ and $\hat{\zeta} \equiv 1/2 = \zeta_\parallel$. As a consequence all variables represent powers of length; e.g., t and f are a length^4 and a length^{-2}, respectively.

To leading order in the small contour undulations, the deterministic coarse-grained tension dynamics, described by Eq. (4), together with the microscopic transverse equation of motion, represents a valid reformulation of the constrained Langevin dynamics of a weakly bending rod subject to a putative pre-stress. The PIDE (4) is the basis not only for discussing the tension dynamics itself, but also the starting point for analytical and numerical calculations of the longitudinal and transverse nonlinear response of a weakly bending polymer. It is the purpose of the present part II to treat the former case in detail, while the latter, somewhat more complex case is reserved for a future communication [8]. In Sec. II, we derive detailed solutions to Eq. (4) for idealized experimental protocols involving a representative selection of external fields. The analytical scaling solutions obtained for a semi-infinite polymer suddenly pulled (or released) at its end reveal the nontrivial short-time phenomenon of tension propagation (Sec. III). At long times, the finite contour length comes in as an additional characteristic length scale, which gives rise to additional scaling regimes, discussed in Sec. IV. To make contact with experiments, we finally identify the repercussions of the tension dynamics on pertinent observables like the (projected) end-to-end distance (Sec. V) and comment on novel experimental perspectives brought up by our analysis (Sec. VI).

II. GENERIC LONGITUDINAL DRIVING FORCES

In general, the tension dynamics depends on how the filament is driven externally—i.e., on the boundary and initial conditions imposed on Eq. (4). With the definition of generic experimental force protocols, this section shall provide a framework for the analysis of Eq. (4). We introduce the scenarios *pulling*, *towing*, and *release* and report on existing investigations. Apart from being directly relevant for experiments, we have chosen to consider these scenarios because of two properties that render them attractive from a theoretical perspective. First, they correspond to *sudden* changes of the environment and thus do not introduce an additional delay time scale. Second, since external forces are assumed to act at the ends, these scenarios only change boundary conditions and leave the equations of motion unchanged. In more complicated scenarios that involve forces applied not only at the ends, these problems show up as subproblems. For instance, if a single point force is applied somewhere within the bulk of a polymer, the filament can be partitioned into two sections that perceive the external force only at their ends.

A. Pulling

The polymer is supposed to be free for negative times, such that it is equilibrated under zero tension at time zero; i.e., we require

$$f_< = f(s,t<0) = 0. \quad (7)$$

Then, for positive times the polymer is pulled in the longitudinal direction at both ends with a constant force $\mathfrak{f}$.[2] The corresponding external force density $\mathfrak{f}[\delta(s-L)-\delta(s)]$ provides the boundary conditions for the tension (see, e.g., the longitudinal equation of motion in part I):

$$f(s=0,t>0) = \mathfrak{f}, \quad f(L,t>0) = \mathfrak{f}. \quad (8)$$

Pulling was first considered by Seifert, Wintz, and Nelson [9] (SWN). They predict that a "large" tension spreads within a time t a characteristic length $\ell_\parallel(t) = \ell_{\mathrm{SWN}}(t) \equiv \ell_p^{1/2}(\mathfrak{f}t)^{1/4}$ from the ends into the bulk of the filament. Their analysis neglects bending forces and thermal forces for the dynamics, albeit the self-affine thermal initial conditions are used (*taut-string approximation*). The contribution of Everaers, Jülicher, Ajdari, and Maggs [10] (EJAM) sheds light on the linear response to longitudinal forces. Their simulations established a typical propagation length of $\ell_\parallel(t) = \ell_{\mathrm{EJAM}}(t) \equiv \ell_p^{1/2}t^{1/8}$ for weak forces, which was previously predicted by Morse [11], and made it plausible by scaling arguments. Brochard–Wyart, Buguin, and de Gennes [12] (BBG) proposed a theory for tension propagation claimed to be valid on scales much larger than ℓ_p supposing, however, the weakly bending approximation. A *quasistatic approximation* underlies their analysis, in which the polymer is at any instant of time considered to be equilibrated with the local tension. Applying their results to the situation considered here, tension should propagate a distance $\ell_\parallel(t) \propto \ell_{\mathrm{BBG}}(t) \equiv \ell_p^{1/2}\mathfrak{f}^{3/4}t^{1/2}$.

Naturally, the scaling arguments used to predict the three different scaling regimes did not address the crossover and the range of validity. Below, we show that in fact only two scaling regimes exist.

[1] The parameter θ occurring in the dynamic force extension relation of part I will be set to 1, $\theta=1$, throughout this paper. It describes the effect of sudden changes in persistence length, which will be discussed elsewhere [13].

[2] Throughout, we denote *external* forces or force fields by fraktur letters.

B. Towing

Pulling of a filament can also be studied for time-dependent external forces. A dynamic force protocol of particular experimental relevance is given by the constant-velocity ensemble: The polymer is pulled by a time-dependent external force $\mathfrak{f}(t)$ at the left end such that this end moves with a *constant velocity* v (towing). Besides the growth law of the boundary layer, we wish to understand the time dependence of the external force. We will see that both quantities are proportional to each other because the external force essentially has to drag a polymer section of length $\ell_\parallel(t)$ through the viscous solvent with the constant velocity v; hence, $\mathfrak{f}(t) \simeq \hat{\zeta} v \ell_\parallel(t)$. By measuring the time-dependent force in a constant-velocity experiment one can thus directly monitor $\ell_\parallel(t)$. Possible experimental realizations are outlined in Sec. VI.

The external force density field corresponding to towing is given by $-\mathfrak{f}(t)\delta(s)$ with an external force $\mathfrak{f}(t)$ determined to fulfill the requirement that $\partial_t r_\parallel(0,t)=v$. Recall from the equations of motion derived in part I, that, up to terms of order $O(\epsilon)$, the gradient of the tension is given by the longitudinal friction (as in a rigid rod). This implies the boundary condition

$$\partial_s f(s=0,t>0) = -\hat{\zeta} v + O(\epsilon), \quad f(L,t>0) = 0. \tag{9}$$

C. Release

Release refers to the process "inverse" to pulling: the filament is supposed to be equilibrated at $t=0$ under a constant pulling force,

$$f_< = f(s,t<0) = \mathfrak{f} > 0. \tag{10}$$

Then, at $t=0$, the external force is suddenly switched off and the filament begins to relax. The ends are considered to be free for $t>0$,

$$f(s=0,t>0) = 0, \quad f(L,t>0) = 0. \tag{11}$$

Release has been discussed by Brochard *et al.* [12]. According to that work the characteristic size of the boundary layer, where the tension is appreciably decreased from $\mathfrak{f}$, should be given by $\ell_\parallel(t) \propto \ell_{\mathrm{BBG}}(t)$ (the same as for pulling).

Furthermore, Brochard *et al.* predict that the tension is relaxed as soon as the tension has spread over the whole filament, yielding a relaxation time $t_L^\parallel$ for the tension that satisfies $\ell_\parallel(t_L^\parallel)=L$. This is in conflict with what we will find Sec. IV, where we identify a novel scaling regime of homogeneous tension relaxation.

III. TENSION PROPAGATION

To unravel the physical implications of Eq. (4) for the scenarios introduced above, we begin with the tension propagation regime $\ell_\parallel \ll L$, where the total length L of the polymer is irrelevant. In this regime, it is legitimate to discuss the dynamics on a (formally) semi-infinite arc length interval $[0,\infty[$. Problems like pulling and release still depend on four independent length scales $(\ell_p, \mathfrak{f}^{-1/2}, s, t^{1/4})$. Yet it is shown in Sec. III A that Eq. (4) is *solved exactly* by a tension profile that obeys a crossover scaling form depending on only two arguments, which can be identified as a reduced time and arc length variable, respectively. In Sec. III B, we then argue that for asymptotically short $(<)$ and long $(>)$ times the scaling function reduces to a function of only one scaling variable $\xi^{\gtrless} = s/\ell_\parallel^{\gtrless}(t)$. Our major results concerning tension propagation, particularly our classification of tension propagation laws $\ell_\parallel^{\gtrless}(t)$, are summarized in Sec. III C.

A. Scaling forms

For each of the generic problems introduced in Sec. II, we shall see that the tension profile obeys certain crossover scaling forms that cannot be inferred from dimensional analysis. These scaling forms greatly simplify the further analysis of the tension dynamics by reducing the number of independent parameters.

To solve the equation of motion, Eq. (4), for a given force protocol, we proceed in the following way. A scaling ansatz is postulated and shown to eliminate the parameter dependence in Eq. (4) and the boundary conditions after a suitable choice of length, time, and force scales. These crossover scales turn out to separate two different regimes: a short- and long-time regime, respectively.[3]

Although being ultimately interested in the tension profile $f(s,t)$, it is convenient to first discuss the *time-integrated* tension $F(s,t)$, defined in Eq. (2), because the equation of motion for the tension, Eq. (4), is naturally formulated in terms of $F(s,t)$. The physically more intuitive quantity $f(s,t)=\partial_t F(s,t)$ is extracted afterwards by a differentiation with respect to time.

We make the following ansatz for the time integral $F(s,t)$ of the tension:

$$F(s,t) = \mathfrak{f} t_\mathfrak{f} \phi\left(\frac{s}{s_\mathfrak{f}}, \frac{t}{t_\mathfrak{f}}\right), \tag{12}$$

in terms of as yet unknown crossover time and length scales $t_\mathfrak{f}$ and $s_\mathfrak{f}$ to be determined below. While a force scale $\mathfrak{f}$ is given explicitly in the case of pulling and release by the pulling and prestretching force, a natural force scale

$$\mathfrak{f} \equiv \hat{\zeta} v s_\mathfrak{f} \quad \text{(towing)} \tag{13}$$

for towing is provided not unless $s_\mathfrak{f}$ is fixed. The combination of variables in Eq. (13) represents the force necessary to drag a polymer section of length $s_\mathfrak{f}$ (longitudinally) through the fluid with the imposed towing velocity v.

As long as the polymer is in equilibrium, $t<0$, the dimensionless scaling function $\phi(\sigma,\tau)$ for the integrated tension is zero for both pulling scenarios, but linearly increasing with time for release due to the constant prestretching force,

[3] Such a crossover was also found in part I for the stored length under a spatially constant tension from ordinary perturbation theory.

$$\phi(\sigma,\tau<0)\equiv c\tau=\begin{cases}0, & \text{pulling and towing},\\ \tau, & \text{release}.\end{cases} \tag{14}$$

The constant c entering the initial condition, Eq. (14), is given by $c=0$ for pulling and towing and $c=1$ for release, respectively.

Since we expect that the signal of a sudden change at the end of the polymer—i.e., at $\sigma=0$—takes time to propagate into the bulk of the polymer, which corresponds to $\sigma\to\infty$, we look for solutions that have a time-independent stored length at $\sigma\to\infty$. According to Eq. (1), this corresponds to the boundary condition of a vanishing curvature of the tension profile at infinity,

$$\partial_\sigma^2\phi(\sigma\to\infty,\tau>0)=0. \tag{15}$$

At the origin, the force and the gradient of the force, respectively, are prescribed by the considered experimental setup,

$$\phi(\sigma=0,\tau>0)=\begin{cases}\tau, & \text{pulling},\\ 0, & \text{release},\end{cases} \tag{16a}$$

$$\partial_\sigma\phi(\sigma=0,\tau>0)=-\tau, \qquad \text{towing}. \tag{16b}$$

Inserting the scaling ansatz, Eq. (12), into Eq. (4) yields after the variable substitutions $q\to q\sqrt{\mathfrak{f}}$, $t\to\tau t_\mathfrak{f}$, and $\tilde{t}\to\tilde{\tau}t_\mathfrak{f}$

$$\ell_p\frac{\mathfrak{f}^{3/2}t_\mathfrak{f}}{\hat{\zeta}s_\mathfrak{f}^2}\partial_\sigma^2\phi(\sigma,\tau) = \int_{-\infty}^{\infty}\frac{dq}{2\pi}\left\{\frac{1}{q^2+c}[1-e^{-2q^2[q^2\tau+\phi(\sigma,\tau)]t_\mathfrak{f}\mathfrak{f}^2}] - 2q^2t_\mathfrak{f}\mathfrak{f}^2\int_0^\tau d\tilde{\tau}e^{-2q^2[q^2(\tau-\tilde{\tau})+\phi(\sigma,\tau)-\tilde{\tau}\phi(\sigma,\tilde{\tau})]t_\mathfrak{f}\mathfrak{f}^2}\right\}. \tag{17}$$

By fixing the scales $t_\mathfrak{f}$ and $s_\mathfrak{f}$ appropriately,

$$t_\mathfrak{f}=\mathfrak{f}^{-2}, \tag{18a}$$

$$s_\mathfrak{f}=\hat{\zeta}^{-1/2}\ell_p^{1/2}\mathfrak{f}^{-1/4}, \tag{18b}$$

we can eliminate the parameter dependence of Eq. (17),

$$\partial_\sigma^2\phi(\sigma,\tau)=\int_{-\infty}^{\infty}\frac{dq}{2\pi}\left\{\frac{1}{q^2+c}[1-e^{-2q^2[q^2\tau+\phi(\sigma,\tau)]}] - 2q^2\int_0^\tau d\hat{\tau}e^{-2q^2[q^2(\tau-\hat{\tau})+\phi(\sigma,\tau)-\phi(\sigma,\hat{\tau})]}\right\}. \tag{19}$$

Note that for towing, the conditions in Eqs. (18a) and (18b) imply the scales

$$t_\mathfrak{f}=(v^2\hat{\zeta}\ell_p)^{-4/5}, \tag{20a}$$

$$s_\mathfrak{f}=(v\hat{\zeta}^3\ell_p^{-2})^{-1/5} \quad \text{(towing)}, \tag{20b}$$

since $\mathfrak{f}$ depends on $s_\mathfrak{f}$ via Eq. (13).

B. Asymptotic scaling

We have thus removed the parameter dependence of the differential equation as well as the boundary and initial conditions. The remaining task is to solve Eq. (19) for ϕ under the initial and boundary conditions given by Eqs. (14)–(16) and to extract the tension

$$f(s,t)=\partial_t F(s,t) \tag{21a}$$

$$=\mathfrak{f}\varphi\left(\frac{s}{s_\mathfrak{f}},\frac{t}{t_\mathfrak{f}}\right) \tag{21b}$$

in terms of the scaling function

$$\varphi(\sigma,\tau)\equiv\partial_\tau\phi(\sigma,\tau). \tag{22}$$

Although this remaining task of finding a solution is analytically not possible in general, we now know, at least, that it should be a function of only two variables: an effective space and time variable $\sigma=s/s_\mathfrak{f}$ and $t_\mathfrak{f}$, respectively. From the conditions in Eqs. (18a) and (18b), it is seen that the scales $s_\mathfrak{f}$ and $t_\mathfrak{f}$ are given by a combination of the characteristic force scale $\mathfrak{f}$ (a length^{-2} in our units) and the persistence length, and hence not simply a consequence of dimensional analysis. The significance of these nontrivial scales is that they mark a crossover in the behavior of the tension. For it turns out that the two-parameter scaling form $\varphi(\sigma,\tau)$ collapses onto the one-parameter scaling form in the limit of large and small arguments—i.e.,

$$\varphi(\sigma,\tau)\to\tau^\alpha\hat{\varphi}\left(\frac{\sigma}{\tau^z}\right), \quad \text{for } \tau\gtrless 1, \tag{23}$$

with a positive and monotonous scaling function $\hat{\varphi}(\xi)$ that is bounded as $\xi\to\{0,\infty\}$ and exponents α and z depending on the problem and the limit—i.e., short- or long-time limit. Equation (23) expresses the asymptotic self-similarity of the tension profile: by stretching the tension profile at a given time in the arclength coordinate σ one obtains the tension profile at a later time, a property inherited from the self-affine conformational fluctuation spectrum of the weakly bending wormlike chain.

Rewriting the scaling variable in Eq. (23) as $\sigma/\tau^z\equiv s/\ell_\parallel(t)$ identifies the tension propagation length

$$\ell_\parallel(t)=s_\mathfrak{f}\left(\frac{t}{t_\mathfrak{f}}\right)^z. \tag{24}$$

In Table I the actual growth laws $\ell_\parallel(t)$ are tabulated depending on the problem and the asymptotic limit.

Before deriving these growth laws from an asymptotic analysis of Eq. (19), let us give a simple argument as to what the exponent z should be at short times. As usual, we assume the crossover should occur when the scaling variable σ/τ^z is of order one; hence,

$$\ell_\parallel^{\gtrless}(t_\mathfrak{f})\asymp s_\mathfrak{f}. \tag{25}$$

If we further assume that at very short times the propagation length $\ell_\parallel^<(\tau)$ of the tension should actually be independent of the external force, we can immediately infer

$$\ell_{\parallel}^{<}(t) \propto \ell_p^{1/2} t^{1/8}, \tag{26}$$

which is the correct short-time growth law, as will be shown in Sec. III B 1.

The derivations we present in the following are consistent in the sense that we use assumptions that are *a posteriori* legitimized by the solutions. In particular, we exploit Eq. (23) as a scaling ansatz in order to derive asymptotic differential equations for the tension. Those equations are then shown to be indeed solved by similarity solutions of the postulated type. In addition, let us assume that the exponent α in Eq. (23) is larger than $-1/2$,

$$\alpha > -1/2; \tag{27}$$

i.e., the tension should increase (decrease) less rapidly than $\tau^{-1/2}$ for $\tau \to 0$ ($\tau \to \infty$). The assumption is reasonable for pulling, because at the ends, we have $\varphi(0,\tau)=1$ and therefore $\alpha=0$ in this case. It turns out that Eq. (27) is correct for all considered problems of tension propagation except for sudden temperature changes, discussed in Ref. [13]. As a consequence, the approximations that are made in the following do not apply to sudden changes in persistence length, which is an indication that it is an exceptional problem. In Sec. IV, where we consider the scaling regime *succeeding* tension propagation, we encounter an asymptotic regime of release characterized by an exponent $\alpha=-2/3$ as another important exception of Eq. (27).

Since the central PIDE (19) is expressed in terms of the time-integrated tension $\phi(\sigma,\tau)$, it is useful for the following discussion to reformulate the scaling assumption, Eq. (23), in terms of ϕ,

$$\phi(\sigma,\tau) \to \tau^{\alpha+1} \hat{\phi}\left(\frac{\sigma}{\tau^z}\right), \quad \text{for } \tau \gtrless 1. \tag{28}$$

1. Short times ($t \ll t_f$)

In case Eq. (27) holds we can linearize Eq. (19) for short times in ϕ. This is at first sight only correct for small wave numbers that satisfy $q^2\phi = O(q^2\tau^{\alpha+1}) \ll 1$. However, upon a closer inspection of the region of large wave vectors, $q > \tau^{-(\alpha+1)/2}$, that do not allow for a linearization, it is seen that there is another term in the exponent, $q^4\tau > \tau^{-2\alpha-1} \gg 1$ (for $\tau \ll 1$ and $\alpha > -1/2$), which renders the considered exponential essentially zero. Therefore, we can approximate Eq. (19) by

$$\begin{aligned}
&\partial_\sigma^2 \phi(\sigma,\tau) \\
&\quad \approx \int_{-\infty}^{\infty} \frac{dq}{2\pi} \left\{ \frac{1}{q^2+c} \{1 - [1 - 2q^2\phi(\sigma,\tau)] e^{-2q^4\tau}\} \right. \\
&\qquad \left. - 2q^2 \int_0^\tau d\hat{\tau} \{1 - 2q^2[\phi(\sigma,\tau) - \phi(\sigma,\hat{\tau})]\} e^{-2q^4(\tau-\hat{\tau})} \right\} \\
&\quad = \int_{-\infty}^{\infty} \frac{dq}{2\pi} \left\{ -\frac{c}{q^2(q^2+c)} (1 - e^{-2q^4\tau}) \right. \\
&\qquad \left. + 2\phi(\sigma,\tau) \left[1 - \left(\frac{c}{q^2+c} \right) e^{-2q^4\tau} \right] \right. \\
&\qquad \left. - 4q^4 \int_0^\tau d\hat{\tau} \phi(\sigma,\hat{\tau}) e^{-2q^4(\tau-\hat{\tau})} \right\}.
\end{aligned} \tag{29}$$

Since $\tau \ll 1$, we can neglect the parameter c in the denominator of the first term and set the exponential function in the second term equal to 1. Furthermore, we observe that the lower bound of the time integral can be set to $-\infty$ by defining $\phi(\sigma,\tau<0) \equiv 0$. After the variable substitution $\hat{\tau} \to \hat{\tau} + \tau$ we obtain

$$\begin{aligned}
\partial_\sigma^2 \phi(\sigma,\tau) = \int_{-\infty}^{\infty} \frac{dq}{\pi} \left[c \frac{e^{-2q^4\tau} - 1}{2q^4} + \frac{q^2 \phi(\sigma,\tau)}{q^2+c} \right. \\
\left. - 2q^4 \int_{-\infty}^0 d\hat{\tau} \phi(\sigma, \hat{\tau} + \tau) e^{2q^4\hat{\tau}} \right].
\end{aligned} \tag{30}$$

Now we introduce the Laplace transform of ϕ according to

$$\phi(\sigma,z) \equiv \int_0^\infty d\tau e^{-z\tau} \phi(\sigma,\tau), \tag{31a}$$

$$\phi(\sigma,\tau) = \int_{c-i\infty}^{c+i\infty} \frac{dz}{2\pi i} e^{z\tau} \phi(\sigma,z), \tag{31b}$$

such that Eq. (30) in Laplace space reads

$$\begin{aligned}
\partial_\sigma^2 \phi(\sigma,z) &= \int_{-\infty}^{\infty} \frac{dq}{\pi} \left[-\frac{c}{2q^4} \left(\frac{1}{z} - \frac{1}{z+2q^4} \right) + \frac{q^2 \phi(\sigma,z)}{q^2+c} \right. \\
&\quad \left. - \int_0^\infty d\tau e^{-z\tau} \int_{-\infty}^0 d\hat{\tau} \phi(\sigma, \hat{\tau} + \tau) (2q^4) e^{2q^4\hat{\tau}} \right] \\
&= \int_{-\infty}^{\infty} \frac{dq}{\pi} \left[-\frac{c}{z(z+2q^4)} + \frac{z\phi(\sigma,z)}{2q^4+z} - \frac{c\phi(\sigma,z)}{q^2+c} \right] \\
&= 2^{-3/4}(z^{1/4}\phi - cz^{-7/4}) - c^{1/2}\phi.
\end{aligned} \tag{32}$$

In the short-time limit $z \gg 1$, this reduces to

$$\partial_\sigma^2 \phi(\sigma,z) = 2^{-3/4} z^{1/4} \phi. \tag{33}$$

Choosing the decaying solution we find for the boundary conditions in Eqs. (15) and (16a) of pulling

$$\phi = \phi_P(\sigma,z) \equiv z^{-2} e^{-\sigma(z/8)^{1/8}} \quad \text{(pulling)}. \tag{34}$$

Since Eq. (32) is a linear differential equation, we can express the solutions for the boundary conditions of towing and release in terms of ϕ_P,

$$\phi = z^{-2} - \phi_P(\sigma,\tau) \quad \text{(release)}, \tag{35a}$$

$$\phi = \int_\sigma^\infty d\hat{\sigma} \phi_P(\hat{\sigma},\tau) \quad \text{(towing)}. \tag{35b}$$

Ultimately, we are interested in the tension

$$\varphi_P(\sigma,\tau) = \partial_\tau \phi_P(\sigma,\tau), \tag{36}$$

which is given by the inverse Laplace transform of $z\phi_P(\sigma,z)$,

$$\varphi_P(\sigma,\tau) = \hat{\varphi}_P\left(\frac{\sigma}{\tau^{1/8}} \right), \tag{37}$$

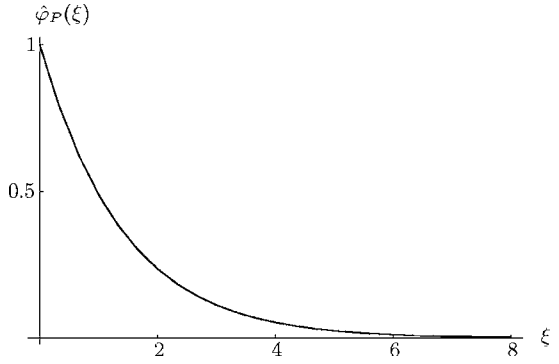

FIG. 1. The scaling function $\hat{\varphi}_P(\xi)$ describing the shape of the tension profile of pulling on short times.

$$\hat{\varphi}_P(\xi) = \int_{-i\infty+\epsilon}^{i\infty+\epsilon} \frac{dz}{2\pi i z} e^{-\xi(z/8)^{1/8}+z}. \tag{38}$$

After deforming the contour of integration such that it encloses the branch cut at the negative real axis, the integral in Eq. (38) becomes

$$\hat{\varphi}_P(\xi) = \int_0^\infty \frac{dx}{\pi} \frac{8}{x} \sin\left[\xi x \sin\frac{\pi}{8}\right] e^{-\xi x \cos(\pi/8)}(1 - e^{-8x^8}), \tag{39}$$

which is to our knowledge not tabulated, but can be easily evaluated numerically; see Fig. 1. Upon using the known Laplace transform,

$$\frac{\Gamma(\nu)}{z^\nu} = \int_0^\infty d\tau e^{-z\tau}\tau^{\nu-1}, \quad \mathrm{Re}\ \nu > 0, \tag{40}$$

and Taylor expanding the integrand of Eq. (38) one obtains an expansion of $\varphi_P(\xi)$ that is particular useful for small ξ,

$$\hat{\varphi}_P(\xi) = \sum_{\substack{n=0 \\ n/8 \notin \mathbb{N}}}^{\infty} \frac{(-2^{-3/8}\xi)^n}{n!\,\Gamma(1-n/8)}. \tag{41}$$

With an absolute error less than 1% the scaling function is approximated by an exponential,

$$\hat{\varphi}_P(\xi) \approx \exp\left(-\frac{\xi}{2^{3/8}\Gamma(7/8)}\right), \tag{42}$$

where the prefactor of ξ in the exponent is the initial slope $\partial_\xi \hat{\varphi}|_{\xi=0}$ of the scaling function.

The tension profiles of the problems under consideration are all related to the scaling function $\hat{\varphi}_P(\xi)$,

$$f(s,t) = \mathfrak{f}\hat{\varphi}_P\left(\frac{s}{\ell_\parallel(t)}\right) \quad \text{(pulling)}, \tag{43a}$$

$$f(s,t) = \mathfrak{f}\left[1 - \hat{\varphi}_P\left(\frac{s}{\ell_\parallel(t)}\right)\right] \quad \text{(release)}, \tag{43b}$$

$$f(s,t) = \hat{\zeta} v \ell_\parallel(t) \int_{s/\ell_\parallel(t)}^\infty d\xi \hat{\varphi}_P(\xi) \quad \text{(towing)}, \tag{43c}$$

where the boundary layer at time t has the typical size

$$\ell_\parallel(t) = \hat{\zeta}^{-1/2}\ell_p^{1/2}t^{1/8} \propto \ell_{\mathrm{EJAM}}(t). \tag{44}$$

The scaling was anticipated in Eq. (26) and in an *ad hoc* scaling argument presented in part I. The result for towing, Eq. (43c), shows that the force at the grafted end, at $\xi=0$, scales like $\hat{\zeta} v \ell_\parallel(t)$. This scaling will be shown to hold also in the long-time limit and can be understood in the sense that the graft has to balance only the drag arising within the boundary layer, since the bulk of the filament is not moving longitudinally. Thus, measuring the force at the grafted end, we can monitor the spreading of the tension. This gives special experimental relevance to the towing scenario. In particular, we predict

$$f(0,t) = \hat{\zeta} v \ell_\parallel(t) 2^{3/8}/\Gamma(9/8) \tag{45}$$

for the force at the grafted end at short times, $\tau \ll 1$. The prefactor in Eq. (45) has been found by evaluating the remaining integral in Eq. (43c), which yields a Taylor series very similar to Eq. (41),

$$\int_\xi^\infty d\hat{\xi}\hat{\varphi}_P(\hat{\xi}) = 2^{3/8} \sum_{\substack{n=-1 \\ n/8-1 \notin \mathbb{N}}}^{\infty} \frac{(-2^{-3/8}\xi)^{n+1}}{(n+1)!\,\Gamma(1-n/8)}. \tag{46}$$

2. Long times ($t \gg t_\dagger$)

The present subsection deals with the dynamics of the tension on a semi-infinite filament at asymptotically long times. We identify and interpret the terms dominating the stored length release in this limit. Neglecting subdominant terms in the continuity equation (1) results in differential equations that can be solved by similarity solutions.

The right-hand side of the nondimensionalized PIDE (19) represents the negative change of stored length in adapted units. It can be written as the sum of two terms A and B, where

$$A \equiv \int_{-\infty}^{+\infty} \frac{dq}{2\pi} \frac{1}{q^2+c}[1 - e^{-2q^2[q^2\tau+\phi(\sigma,\tau)]}], \tag{47a}$$

$$B \equiv -\int_{-\infty}^{\infty} \frac{dq}{2\pi} 2q^2 \int_0^\tau d\hat{\tau} e^{-2q^2[q^2(\tau-\hat{\tau})+\phi(\sigma,\tau)-\phi(\sigma,\hat{\tau})]}. \tag{47b}$$

We already pointed out in part I that the term A can be interpreted as the "deterministic relaxation" of stored length (for the fictitious situation "$T=0$"—i.e., no thermal noise—for $t>0$). The term B describes the increase in stored length due to the thermal kicks and is strictly positive. We analyze both terms separately.

For prestretched initial conditions ($c=1$) the long-time limit of A follows from setting the exponential to zero,

$$A \overset{\tau\gg 1}{\to} \int_{-\infty}^{+\infty} \frac{dq}{2\pi} \frac{1}{q^2+1} = \frac{1}{2}, \quad \text{for } c=1. \tag{48}$$

The term A for $\tau\to\infty$ is nothing but the initially stored length, which is completely relaxed after a purely deterministic relaxation.

The same reasoning cannot be applied in cases of a tension-free initial state (both pulling problems): setting the exponential to zero in Eq. (47a) for $c=0$ yields an infrared divergence. The exponential has to be retained to render the integrand finite at small wave numbers. For the dominant small wave numbers one can, however, neglect the term $2q^4\tau$ in the exponent because it is small compared to the term $2q^2\Phi$, so that we arrive at the asymptotic expression

$$A \overset{\tau\gg 1}{\to} \int_{-\infty}^{+\infty} \frac{dq}{2\pi} \frac{1}{q^2}[1-e^{-2q^2\phi(\sigma,\tau)}] = \sqrt{\frac{2}{\pi}}\sqrt{\phi(\sigma,\tau)}, \quad \text{for } c=0, \tag{49}$$

i.e., the "deterministic relaxation" is dominated by the tension term and bending can be neglected (as heuristically assumed by Seifert *et al.* [9]). A more formal justification for Eqs. (48) and (49) is given in Appendix A 1.

The term B, describing the stored length generated by the thermal kicks, takes for asymptotically large $\tau\gg 1$ the form

$$B \overset{\tau\gg 1}{\to} -\int_{-\infty}^{\infty} \frac{dq}{2\pi} \frac{1}{q^2+\partial_\tau\phi(\sigma,\tau)} = -\frac{1}{2\sqrt{\partial_\tau\phi(\sigma,\tau)}}, \tag{50}$$

independent of the initial conditions. This is shown in Appendix A 2 upon using the scaling assumptions in Eqs. (28) and (27). The result, Eq. (50), should not come as a surprise. It simply represents the (negative) stored length of a stiff polymer equilibrated at the (rescaled) tension $\partial_\tau\phi$. For a constant force—i.e., $\partial_\tau\phi$=const.—it is obvious that the stored length should saturate for long times at the corresponding equilibrium value. But also if the tension is varying slowly enough in time ($\alpha>-1/2$), the "noise-generated" stored length can be considered as quasistatically equilibrated with the tension.

Finally, we combine the "relaxed stored length" expressed in A and the "noise-generated stored length" B.

a. Pulling and towing. For $c=0$ and $\alpha>-1/2$ the term $A\propto\sqrt{\phi}\propto\tau^{\alpha/2+1/2}$ is much larger than $B\propto(\partial_\tau\phi)^{-1/2}=O(\tau^{-\alpha/2})$, i.e., the effects of noise can be neglected on long times (as presumed by Seifert *et al.* [9]). In this limit, the thermal noise is merely relevant in preparing the initial state. The relaxation after force application for $\tau\gg 1$ is purely mechanical, like for a pulled string that is initially prepared with some contour roughness (taut-string approximation). If we replace the right-hand side of Eq. (19) by the asymptotic form of A, Eq. (49), we obtain the partial differential equation

$$\partial_\sigma^2\phi(\sigma,\tau) = \sqrt{\frac{2}{\pi}}\sqrt{\phi(\sigma,\tau)} \tag{51}$$

for the dynamics of the integrated tension ϕ.

Equation (51) represents a Newtonian equation of motion for a particle moving in a conservative force field $\propto\sqrt{\phi}$ and can be integrated straightforwardly. In the case of pulling the solution, which satisfies the boundary conditions in Eqs. (15) and (16a) of pulling [in particular $\phi(0,\tau)=\tau$], is given by

$$\phi(\sigma,\tau) = \tau[\sigma/(72\pi\tau)^{1/4}-1]^4 \tag{52}$$

for $\sigma<(72\pi\tau)^{1/4}$ and $\phi=0$ otherwise. The dimensionless tension φ is derived from ϕ via differentiation [see Eq. (22)] and obeys a scaling form

$$f(s,t) = \mathfrak{f}\varphi(s,t) = \mathfrak{f}\hat{\varphi}\left(\frac{s}{\ell_\parallel(t)}\right), \tag{53}$$

with a typical boundary layer size proportional to $\ell_{\mathrm{SWN}}(t)$,

$$\ell_\parallel(t) = t^{1/4}\hat{\zeta}^{-1/2}\ell_p^{1/2}\mathfrak{f}^{1/4}, \tag{54}$$

and a scaling function $\hat{\varphi}$ given by

$$\hat{\varphi}(\xi) = [1-\xi/(72\pi)^{1/4}]^3 \tag{55}$$

for $\xi<(72\pi)^{1/4}$ and $\hat{\varphi}=0$ otherwise. Towing starts with the same initial conditions ($c=0$) but with different boundary conditions, Eqs. (15) and (16b). Again, we have to solve Eq. (51), but now under the boundary condition $\partial_\sigma\phi(0,\tau)=-\tau$. The solution is

$$\phi(\sigma,\tau) = \tau^{4/3}\left(\frac{9\pi}{32}\right)^{1/3}\left[\frac{\sigma}{(18\pi\tau)^{1/3}}-1\right]^4 \tag{56}$$

for $\sigma<(18\pi\tau)^{1/3}$ and $\phi=0$ otherwise. This implies a tension profile of

$$f(s,t) = \hat{\zeta}v\ell_\parallel(t)\hat{\varphi}\left(\frac{s}{\ell_\parallel(t)}\right), \tag{57}$$

with the typical boundary layer size

$$\ell_\parallel(t) = t^{1/3}\ell_p^{2/3}(v/\hat{\zeta})^{1/3} \tag{58}$$

and the scaling function $\hat{\varphi}$ given by

$$\hat{\varphi}(\xi) = \left(\frac{2\pi}{3}\right)^{1/3}[1-\xi/(18\pi)^{1/3}]^3 \tag{59}$$

for $\xi<(18\pi)^{1/3}$ and $\hat{\varphi}=0$ otherwise. As at short times, the absolute value of the reduced tension at the left end is proportional to the size of the boundary layer. Its precise value is predicted to be

$$f(0,t) = (2\pi/3)^{1/3}\hat{\zeta}v\ell_\parallel(t) \propto t^{1/3} \tag{60}$$

and should be directly accessible to single molecule experiments.

b. Release. The stored length release is asymptotically given by

$$-\langle\Delta\bar{\varrho}\rangle \propto A+B \overset{\tau\gg 1}{\sim} \frac{1}{2} - \frac{1}{2\sqrt{\partial_\tau\phi(\sigma,\tau)}}. \tag{61}$$

This expression for the change in stored length can also be directly obtained if one assumes that the filament was at any time equilibrated with the current tension $\varphi=\partial_\tau\phi$ (*quasistatic approximation*). Our derivations show that this assumption, used by Brochard-Wyart *et al.* [12], is only valid in the long-

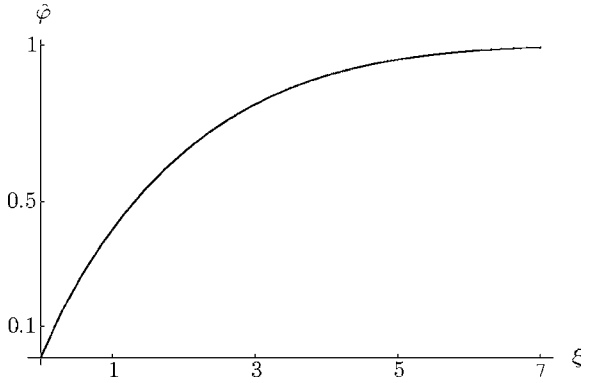

FIG. 2. The scaling function $\hat{\varphi}(\xi)$ for release obtained by a numerical solution of Eq. (66).

time limit for the scenario of release. The dynamics of the integrated tension is then described by

$$\partial_\sigma^2 \phi = \frac{1}{2} - \frac{1}{2\sqrt{\partial_\tau \phi(\sigma,\tau)}} \tag{62}$$

or, in terms of the tension $\varphi = \partial_\tau \phi(\sigma,\tau)$,

$$\partial_\sigma^2 \varphi = \frac{1}{4}\varphi^{-3/2}\partial_\tau \varphi. \tag{63}$$

The solution satisfying the correct boundary conditions, Eqs. (15) and (16a), is given by a scaling form

$$\varphi(s,t) = \hat{\varphi}\left(\frac{s}{\ell_\parallel(t)}\right), \tag{64}$$

with the typical boundary layer size now growing like

$$\ell_\parallel(t) = t^{1/2}\hat{\zeta}^{-1/2}\ell_p^{1/2}\mathfrak{f}^{3/4} \propto \ell_{\mathrm{BBG}}(t) \tag{65}$$

and a scaling function $\hat{\varphi}(\xi)$ satisfying the ordinary differential equation

$$\partial_\xi^2 \hat{\varphi} = -\frac{1}{8}\xi\hat{\varphi}^{-3/2}\partial_\xi \hat{\varphi}. \tag{66}$$

The scaling function depicted in Fig. 2 was already obtained numerically in Ref. [12]. The slope at the origin is $\partial_\xi \hat{\varphi}|_{\xi=0} \approx 0.6193$.

C. Tension propagation (summary)

This section summarizes the picture of tension propagation that emerges from the above solutions of the dynamical equation for the tension, Eq. (4), for sudden changes in boundary conditions.

For the considered problems pulling, towing, and release, we have shown that the tension profile in units of $\mathfrak{f}$ has to obey a crossover scaling form $\varphi(\sigma,\tau)$ depending on a reduced time variable $\tau \equiv t/t_\mathfrak{f}$ and a reduced arc length variable $\sigma \equiv s/s_\mathfrak{f}$. The scaling function φ describes how sudden changes of the tension at the ends spread into the bulk of the polymer. Its crossover structure and the expressions for $t_\mathfrak{f}$ and $s_\mathfrak{f} \approx \ell_\parallel(t_\mathfrak{f})$ are consistent with our heuristic discussion of pulling in part I. In the limits $\tau \ll 1$ and $\tau \gg 1$ the function $\varphi(\sigma,\tau)$ assumes a simple (one-variable) scaling form

$$\varphi \sim \tau^{\alpha_\gtrless}\hat{\varphi}^{\gtrless}[\sigma/\tau^{z_\gtrless}]. \tag{67}$$

The notation $\gtrless$ indicates that the asymptotic form of $\hat{\varphi}$, α, and z will generally not only depend on the kind of external perturbation applied, but will also differ for times $t \gtrless t_\mathfrak{f}$. Rewriting $\sigma/\tau^z \equiv s/\ell_\parallel$ identifies the tension propagation length $\ell_\parallel \equiv s_\mathfrak{f}\,\tau^z$.

For $t \ll t_\mathfrak{f}$, Eq. (4) could be linearized in f and the scaling function $\hat{\varphi}^<$ was obtained analytically. Whereas $\hat{\varphi}^<$ depends on the considered force protocol, the corresponding exponent $z_< = 1/8$ is independent of the boundary conditions. As established by our heuristic discussion of pulling, this is due to the relaxation of modes with Euler forces $\ell_\perp^{-2} \gg \mathfrak{f}$ much larger than the external force, for which the equilibrium-mode spectrum is hardly perturbed by the external force. The self-affinity of the equilibrium-mode spectrum translates into a self-similar relaxation dynamics. The dynamic exponent z for the growth of the boundary layer could already be anticipated from requiring $\hat{\varphi}^<$ to become $\mathfrak{f}$ independent as in linear response; see Eq. (26). The short-time dynamics for strong external force is thus closely related to the linear response. Note, however, that the limit $\mathfrak{f} \to 0$ is problematic, as it does not interchange with $\epsilon \to 0$. Our identification of arclength averages with (local) ensemble averages in part I breaks down for $\mathfrak{f} < (\zeta/\ell_p)^{1/4} t^{-7/16}$, where fluctuations in the tension become comparable to its average value. In fact, extending Eq. (4) to linear response amounts to an uncontrolled factorization approximation $\langle f r_\perp^2 \rangle \to \langle f \rangle \langle r_\perp^2 \rangle$. Even in the stiff limit the linear longitudinal dynamic response remains an open problem. The limit where fluctuations in the tension become important and its consequences will be detailed in Sec. V E.

For $t \gg t_\mathfrak{f}$ the dynamics becomes nonlinear in the external force and starts to depend on the kind of external perturbation and on how precisely it is applied to the polymer. Previously predicted power laws were recovered from Eq. (4) by employing different approximations to its right-hand side. In the taut-string approximation of Ref. [9], one neglects for $t > 0$ bending and thermal forces against the tension; i.e., one drops the q^4 term in the relaxation time $\tau_q = q^4 + fq^2$ of a mode with wave number q and sets $\ell_p \to \infty$ for positive times (i.e., $\theta = 0$). The complementary quasistatic approximation of Ref. [12] amounts to the omission of memory effects—i.e., to the assumption of instantaneous equilibration of tension and stored length (as would be the case for vanishing *transverse* friction, $\zeta_\perp \to 0$). In cases where either of these approximations applies, a power-law dispersion relation combines with a self-affine-mode spectrum to produce self-similar tension dynamics. Our analysis of Eq. (4) showed that either of these approximations becomes rigorous in the

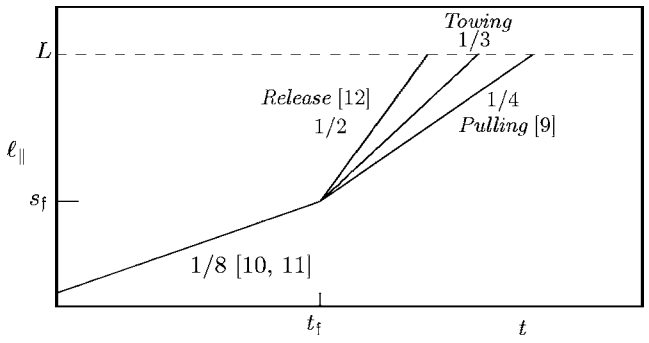

FIG. 3. Schematic of the tension propagation laws $\ell_\parallel(t) \propto t^z$ on a double-logarithmic scale. At $t_\mathfrak{f}=\mathfrak{f}^{-2}$ they cross over from a universal short-time regime to (problem-specific) tension-dominated intermediate asymptotics, except for weak forces, $\mathfrak{f} < \ell_p^2/L^4$. The propagation ends when $\ell_\parallel(t) \approx L$.

intermediate asymptotic regime defined by $t \gg t_\mathfrak{f}$, $\ell_\parallel \ll L$. The quasiequilibrium approximation applies to release and the taut-string approximation to pulling. We could rule out the applicability of the taut-string approximation for release and of the quasistatic approximation for pulling [12] and towing. The "pure" scenarios of self-similar dynamics are summarized in Table I and Fig. 3.

IV. TERMINAL STRESS RELAXATION

Up to now, we have considered the growth of the boundary layer in a stiff polymer that has a (formally) semi-infinite arclength parameter space, $s \in [0, \infty[$, which is an idealization. However, the foregoing discussion obviously applies to a polymer of *finite* length L for sufficiently short times: As long as the size of the boundary layer is much smaller than the total length L the presence of a second end is irrelevant to the boundary layer at the first end. The time where the boundary layers span the whole polymer marks the crossover to a new behavior. For definiteness, we define the crossover time $t_L^\parallel$ by

$$\ell_\parallel(t_L^\parallel) \equiv L. \tag{68}$$

What happens for $t > t_L^\parallel$? The straightforward way to answer this question is to solve for the intermediate asymptotics of the PIDE (4) for a polymer of finite length. The finiteness of L amounts to replacing the boundary condition $\partial_s^2 f(s \to \infty) = 0$ by the correct problem-specific one—i.e., by

$$f(L, t > 0) = \mathfrak{f}, \quad \text{pulling},$$

$$f(L, t > 0) = 0, \quad \text{release, towing}.$$

One could now proceed as in Sec. III B by identifying proper scaling forms and extracting their asymptotic behavior. As compared to the semi-infinite polymer limit, this procedure is more complicated for a finite polymer because of the additional scaling variable $\ell_\perp(t)/L$. Therefore, we prefer to take the following shortcut, which consists in two steps.

(i) *Trivial tension profiles for $t \gg t_\star$.* In the heuristic analysis of part I, we found that ordinary perturbation theory (OPT) should become valid for times larger than some crossover time $t_\star$. With the exception of towing, which we discuss separately below, the introduced scenarios treat both ends equally, such that the tension profile in OPT has a trivial time and arc length dependence—namely,

$$f^{\mathrm{OPT}}(s,t) = f(0,t) = \text{const}, \tag{69}$$

up to small terms of order $O(\epsilon)$. For constant tension we can easily extract the longitudinal dynamics from Eq. (3). The corresponding predictions for the evolution of the end-to-end distance will be discussed in Sec. V B.

(ii) *Possibility of homogeneous tension relaxation for $t_L^\parallel \ll t \ll t_\star$.* Up to now, we have argued that the tension propagates for $t \ll t_L^\parallel$ and is constant in time and space for $t \gg t_\star$. There remains the question whether there is a nontrivial regime of homogeneous tension relaxation in the time interval $[t_L^\parallel; t_\star]$. Using the systematic approach outlined in Appendix C to determine $t_\star$, we actually find for most of the problems that $t_\star \simeq t_L^\parallel$; i.e., there is no scaling regime between tension propagation and the stationary tension profiles dictated by OPT. The release scenario, however, provides an important exception, as it allows for a time-scale separation $t_L^\parallel \ll t_\star$, as we demonstrate explicitly below. For intermediate times the tension relaxation is shown to exhibit a novel behavior with an almost parabolic tension profile and an amplitude that slowly decays in time according to a power law.

Release for large prestretching force

Let us first determine the time $t_\star$, at which OPT becomes valid, for release. In the OPT regime, the tension should be so small that we can calculate the change in stored length accurately by means of Eq. (3) (with the prestretched initial conditions of release—i.e., $f_< = \mathfrak{f}$) under the assumption of a vanishing tension, $f^{\mathrm{OPT}}=0$,

$$\langle \Delta\bar{\varrho} \rangle(t) = \int_0^\infty \frac{dq}{\pi \ell_p} \left\{ \frac{1}{q^2+\mathfrak{f}} (e^{-2q^4 t} - 1) + 2q^2 \int_0^t d\tilde{t} e^{-2q^4(t-\tilde{t})} \right\} \tag{70a}$$

$$= \int_0^\infty \frac{dq}{\pi \ell_p} \left\{ \left(\frac{1}{q^2} - \frac{1}{q^2+\mathfrak{f}} \right) (1 - e^{-2q^4 t}) \right\} \tag{70b}$$

$$= \frac{t^{1/4}}{\ell_p} \int_0^\infty \frac{dq}{\pi} \left\{ \left(\frac{1}{q^2} - \frac{1}{q^2 + \sqrt{t/t_\mathfrak{f}}} \right) (1 - e^{-2q^4}) \right\} \tag{70c}$$

$$\overset{t \gg t_\mathfrak{f}}{\sim} \frac{2^{3/4}}{\Gamma(1/4)} \frac{t^{1/4}}{\ell_p}. \tag{70d}$$

Here, we have substituted $q \to q t^{-1/4}$ and replaced $\mathfrak{f}$ by $t_\mathfrak{f}^{-1/2}$ in order to obtain Eq. (70d). In the final step, we took the long-time limit $t \gg t_\mathfrak{f}$. Let us now determine the order of magnitude of the variation δf of the tension due to the longitudinal friction. Estimating $\delta f \simeq \hat{\zeta} \langle \Delta\bar{\varrho} \rangle / (tL^2)$ from Eq. (1), we obtain

TABLE I. Asymptotic growth laws for the dynamic size $\ell_\parallel(t)$ of the tension boundary layer.

Problem	$t \ll t_\mathfrak{f}$	$t_\mathfrak{f} \ll t \ll t_L^\parallel$
Pulling	$\sqrt{\ell_p/\hat{\zeta}}t^{1/8}$	$\sqrt{\ell_p/\hat{\zeta}\mathfrak{f}}^{1/4}t^{1/4}$
Towing	$\sqrt{\ell_p/\hat{\zeta}}t^{1/8}$	$(\ell_p^2 v/\hat{\zeta})^{1/3}t^{1/3}$
Release	$\sqrt{\ell_p/\hat{\zeta}}t^{1/8}$	$\sqrt{\ell_p/\hat{\zeta}\mathfrak{f}}^{3/4}t^{1/2}$

$$\delta f \approx \hat{\zeta}\frac{L^2}{\ell_p}t^{-3/4}. \tag{71}$$

As in the heuristic discussion of part I, we find a diverging tension in the limit $t \to 0$ for the OPT result, so that the OPT result can only be valid after the effect of δf on the evolution of $\langle \Delta\bar{\varrho}\rangle(t)$ can be neglected. For the particular case of release, this time can be determined as follows. As discussed in part I, the stress-free dynamics is at the time t characterized by relaxation of modes with wavelength $\ell_\perp(t) \simeq t^{1/4}$. When δf is larger than the critical Euler buckling force $\ell_\perp(t)^{-2}$ corresponding to the length $\ell_\perp(t)$ we expect that the tension cannot be neglected for the evolution of $\langle \Delta\bar{\varrho}\rangle$. Hence, the above result $\langle \Delta\bar{\varrho}\rangle \propto Lt^{1/4}/\ell_p$, obtained from OPT, can only be valid if

$$\ell_\perp(t)^2 \delta f \simeq \frac{L^2}{\ell_p}t^{-1/4} \ll 1, \tag{72}$$

i.e., for long enough times

$$t \gg t_\star = L^8/\ell_p^4. \tag{73}$$

The time $t_\star(L)$ is obviously not identical with the time

$$t_L^\parallel = L^2\ell_p^{-1}\hat{\zeta}\mathfrak{f}^{-3/2} \quad (t \gg t_\mathfrak{f}) \tag{74}$$

it takes for the boundary layer to spread over the filament. To compare them, we first notice that $t_L^\parallel \gg t_\mathfrak{f} = \mathfrak{f}^{-2}$ implies that the polymer must have been prestretched by a large enough force,

$$\mathfrak{f} \gg \ell_p^2/L^4 = \epsilon^{-2}L^{-2}, \tag{75}$$

larger than the prestretching force at least necessary to enter the propagation regime $t_\mathfrak{f} \ll t \ll t_L^\parallel$. By using the estimate in Eq. (75) we can compare $t_\star$ and $t_L^\parallel$,

$$t_\star(L) = \frac{L^2}{\ell_p}\left(\frac{L^2}{\ell_p}\right)^3 \gg \frac{L^2}{\ell_p}\mathfrak{f}^{-3/2} \simeq t_L^\parallel. \tag{76}$$

It is seen that the time window $t_L^\parallel \ll t \ll t_\star$ grows with the prestretching force, which means, in particular, that it describes the limit of an initially straight polymer.

To determine the physics of this regime, we have to solve the equation of motion for the tension on the finite arclength interval $[0;L]$ using the approximations developed in Sec. III B. There, we found that in the limit $t \gg t_\mathfrak{f}$ the tension profile of release is described by Eq. (63):

$$\partial_\sigma^2\varphi = \frac{1}{4}\varphi^{-3/2}\partial_\tau\varphi. \tag{77}$$

The right-hand side represents the time derivative of the stored length in the quasistatic approximation. Going back to the variables f, s, and t, Eq. (77) takes the form

$$\partial_s^2 f = \frac{1}{4}\frac{\hat{\zeta}}{\ell_p}f^{-3/2}\partial_t f. \tag{78}$$

For the following, we assume that this quasistatic approximation is not only valid in the tension propagation regime for $t_\mathfrak{f} \ll t \ll t_L^\parallel$, but also for longer times until the OPT regime begins, $t_\mathfrak{f} \ll t \ll t_\star$. This is justified *a posteriori* in Appendix B, where it is shown that the change in stored length for the solution $f(s,t)$ of Eq. (78) can indeed be calculated quasistatically for times $t \ll t_\star$. We solve Eq. (78) for the boundary conditions

$$f(s=0,t) = 0, \quad f(s=L,t) = 0 \tag{79}$$

and the initial conditions

$$f(s,0) = \mathfrak{f}, \quad \text{for } 0 < s < L. \tag{80}$$

In Sec. III B 2, we solved the differential equation (77) with the scaling ansatz $f = \mathfrak{f}\hat{\varphi}[s/\ell_\parallel(t)]$ numerically for the correct initial condition, but ignored the boundary conditions at one end by sending $L \to \infty$. In contrast, we now look for a simple solution that obeys the tension boundary conditions exactly at the expense of a possible mismatch with the initial conditions. To this end, we make the product ansatz

$$f(s,t) = g(t)h(s). \tag{81}$$

Separation of variables yields

$$\frac{\hat{\zeta}}{4\ell_p}g^{-5/2}\partial_t g = C = \sqrt{h}h''. \tag{82}$$

Choosing $C = -1/(6L^2)$, for convenience, we find the long-time asymptotics

$$g(t) \sim \left(\frac{\hat{\zeta}L^2}{\ell_p t}\right)^{2/3}. \tag{83}$$

The spatial part obeys a scaling form $h(s) = \hat{h}(s/L)$, where $\hat{h}$ satisfies the equation

$$\partial_\xi^2\hat{h}(\xi) = -\frac{1}{6}\hat{h}^{-1/2}, \tag{84}$$

with the boundary condition

$$\hat{h}(0) = \hat{h}(1) = 0. \tag{85}$$

The analytical solution can be found in a standard way. The main characteristics are the slope at $\xi = 0$,

$$\partial_\xi h(\xi)|_{\xi=0} = 12^{-1/3} \approx 0.4368, \tag{86}$$

and the maximum value of h,

$$h(1/2) = \frac{1}{16}\left(\frac{3}{2}\right)^{2/3} \approx 0.0819. \tag{87}$$

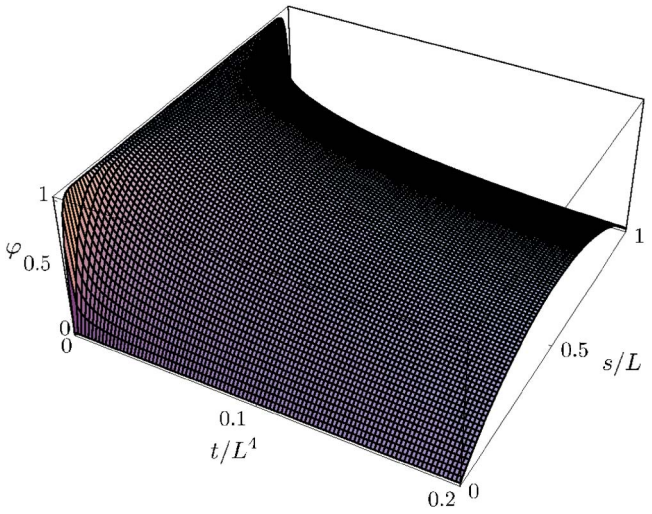

FIG. 4. (Color online) The initial ($t \ll t_\star$) time evolution of release. A regime of (slow) tension relaxation begins after the sudden change in boundary condition has propagated through the filament.

Up to now we have investigated the quasistatic approximation in the tension propagation regime ($t \ll t_L^{\parallel}$) and in the regime of tension relaxation ($t \gg t_L^{\parallel}$) separately. In order to illustrate the crossover, we have also solved the corresponding PIDE (78), numerically. The result shown in Fig. 4 unveils the transient nature of the tension propagation regime.

V. NONLINEAR RESPONSE OF THE PROJECTED LENGTH

After having discussed the rich tension dynamics of stiff polymers in detail, we wish to derive its consequences for pertinent observables in order to make contact with experiments. Although the tension may in some situations be monitored directly (see Sec. VI), a more conventional observable is the longitudinal extension $R_{\parallel}(t)$ of the polymer, which is defined to be the end-to-end distance projected onto the longitudinal axis. Tension dynamics strongly affects the nonlinear response of the projected length, which shall be detailed in the following for the force protocols pulling, towing, and release.

The average temporal change in the projected length $R_{\parallel}(t)$ is directly related to the stored length release,

$$\langle \Delta R_{\parallel} \rangle(t) = -\int_0^L ds \langle \Delta \varrho \rangle(s,t) + o(\epsilon), \tag{88}$$

which was already noted in part I. As long as modes with wavelength on the order of the total length are irrelevant (i.e., both ends of the polymer are not correlated),

$$\ell_\perp(t) \ll L, \tag{89}$$

half-space solutions for $\langle \Delta \varrho \rangle$ may be used to evaluate Eq. (88).

Recall from part I that $\langle \Delta \varrho \rangle$ can be decomposed into a bulk contribution $\langle \Delta \bar{\varrho} \rangle$ and a term influenced by the boundary conditions, which vanish under a spatial average. We show in Sec. V I that in the cases of hinged and clamped ends, as opposed to free ends, the contribution of the boundary term to the integral in Eq. (88) is subdominant in the limit $t \to 0$. Nevertheless, these boundary effects represent important corrections that should be taken into account in any experimental situation (i.e., with finite t) of pulling and towing.

At first, however, let us consider the *bulk* contribution to the end-to-end distance,

$$\langle \Delta \bar{R}_{\parallel} \rangle(t) \equiv \int_0^L ds \langle \Delta \bar{\varrho} \rangle [F(s, \tilde{t} \le t), t], \tag{90}$$

which is universal in the sense that it does not depend on the boundary conditions of $\boldsymbol{r}_\perp$. In Eq. (90) and in the following, we neglect contributions of higher order than $\Delta \varrho = O(\epsilon)$ to the projected end-to-end distance. According to Eqs. (1) and (90), the bulk change of the end-to-end distance is given by the arclength integral of the curvature of the time-integrated tension $F(s,t)$,

$$\langle \Delta \bar{R}_{\parallel} \rangle(t) = \hat{\zeta}^{-1} \int_0^L ds F''(s,t) \tag{91a}$$

$$= \hat{\zeta}^{-1} [F'(L,t) - F'(0,t)]. \tag{91b}$$

The predictions are presented separately for the regime of tension propagation ($t \ll t_L^{\parallel}$) and the regime of OPT ($t \gg t_\star$), where the tension profiles are flat and time independent up to subleading terms. For weak forces, an explicit expression for times $t < t_\star$ is given in Sec. V D, which captures the crossover from tension propagation to the tension-saturated OPT regime. As discussed in Sec. IV, release turns out to also have an additional time window $t_L^{\parallel} < t < t_\star$, whose consequences for the end-to-end distance are described in Sec. V C. Since towing is the only problem, in which both ends do not behave in the same way, we discuss this "asymmetrical" problem separately in Sec. V G.

A. Tension propagation regime ($t \ll t_L^{\parallel}$)

In the time domain of tension propagation, where the boundary layers are growing in from both ends ($t \ll t_L^{\parallel}$), we may use the tension profiles for the semi-infinite (pseudo)polymer from Sec. III A (labeled by F_∞ here) to approximate Eq. (91b) by

$$\langle \Delta \bar{R}_{\parallel} \rangle(t) \overset{t \ll t_L^{\parallel}}{\sim} -2 \hat{\zeta}^{-1} F'_\infty(0,t) \tag{92}$$

for scenarios with *two* equally treated ends. Now, if t falls into a regime where the tension exhibits scaling,

$$F_\infty(s,t) \propto t^{\alpha+1} \hat{F}_\infty\left(\frac{s}{t^z}\right), \tag{93}$$

we immediately obtain from Eq. (92) the power law

$$\langle \Delta \bar{R}_{\parallel} \rangle(t) \propto -t^{\alpha+1-z} 2 \partial_\xi \hat{F}_\infty(\xi = 0) \tag{94}$$

for the growth of the end-to-end distance. The prefactors can be calculated for all cases, because the scaling functions are

TABLE II. Universal bulk contribution $\langle \Delta \bar{R}_{\|} \rangle(t)$ to the dynamic change of the end-to-end distance in the limit $t \ll t_L^{\|} \ll t_L^{\perp}$.

Problem	$t \ll t_{\mathfrak{f}}$	$t \gg t_{\mathfrak{f}}$
Pulling	$[2^{5/8}/\Gamma(15/8)](\mathfrak{f}/\sqrt{\hat{\zeta}\ell_p})t^{7/8}$	$4/\sqrt{3}(2/\pi)^{1/4}(\mathfrak{f}^{3/4}/\sqrt{\hat{\zeta}\ell_p})t^{3/4}$
Release	$-[2^{5/8}/\Gamma(15/8)](\mathfrak{f}/\sqrt{\hat{\zeta}\ell_p})t^{7/8}$	$-2.477(\mathfrak{f}^{1/4}/\sqrt{\hat{\zeta}\ell_p})t^{1/2}$

known. In this way we obtain the list given in Table II of the growth laws.

B. OPT regime ($t \gg t_\star$)

When calculating the release of the stored length in OPT the tension profile $f^{\mathrm{OPT}}=f(s=0)=\mathrm{const}$ is assumed to be stationary and flat, so that

$$\langle \Delta \bar{R}_{\|} \rangle(t) = -L\langle \Delta \bar{\varrho} \rangle[f^{\mathrm{OPT}},t], \quad \text{for } t \gg t_\star. \tag{95}$$

In the case of release, the quantity $\langle \Delta \bar{\varrho} \rangle(f^{\mathrm{OPT}}=0,t)$ has been explicitly calculated in Eq. (70a)–(70d). For pulling, $\langle \Delta \bar{\varrho} \rangle \times (f^{\mathrm{OPT}}=\mathfrak{f},t)$ can be evaluated from Eq. (3) in a similar straightforward manner, because the tension is spatially constant. The corresponding growth laws are summarized in Table III.

Compared to the tension propagation regime, the growth laws in the OPT regime are slowed down; see Tables II and III. Actually, for all cases except release the corresponding growth laws obey [14,15]

$$\langle \Delta \bar{R}_{\|} \rangle^{\mathrm{OPT}} \propto \langle \Delta \bar{R}_{\|} \rangle^{\mathrm{MSPT}} t^{-z}.$$

This can be understood in terms of the scaling arguments used part I. There, we took tension propagation heuristically into account by assuming that the stored length release, as given by OPT, is restricted to the boundary layer of size $\ell_{\|}(t)$. Then, one has

$$\langle \Delta \bar{R}_{\|} \rangle^{\mathrm{OPT}} \simeq -\ell_{\|}(t)\langle \Delta \bar{\varrho} \rangle(f^{\mathrm{OPT}},t) \quad \text{for } t \ll t_L^{\|} \tag{96}$$

as compared to

$$\langle \Delta \bar{R}_{\|} \rangle^{\mathrm{MSPT}} \simeq -L\langle \Delta \bar{\varrho} \rangle(f^{\mathrm{OPT}},t) \quad \text{for } t \gg t_\star. \tag{97}$$

This conforms with the heuristic rule noticed above,

$$\langle \Delta \bar{R}_{\|} \rangle^{\mathrm{OPT}} \approx \frac{L}{\ell_{\|}(t)} \langle \Delta \bar{R}_{\|} \rangle^{\mathrm{MSPT}} \sim t^{\alpha+1-2z}. \tag{98}$$

C. Release in the limit $t_L^{\|} \ll t \ll t_\star$

The intuitive rule in Eq. (98) fails for release in the limit $t \gg t_{\mathfrak{f}}$, which indicates that this is an exceptional scenario. As discussed in Sec. IV, $t_\star = L^8/\ell_p^4$ cannot be identified with $t_L^{\|} = L^2 \ell_p^{-1} \hat{\zeta} \mathfrak{f}^{-3/2}$ in this case. There exists a time window $t_L^{\|} \ll t \ll t_\star$ that expands in the limit of large forces, $\mathfrak{f} \gg \ell_p^2/L^4$. We have shown that the tension exhibits homogeneous relaxation in this regime. With the slope of the tension at the ends,

$$\partial_s f|_{s=\{^0_L\}} = \pm \frac{1}{16}\left(\frac{3}{2}\right)^{2/3} \frac{1}{L}\left(\frac{\hat{\zeta}L^2}{\ell_p t}\right)^{2/3}, \tag{99}$$

the growth law

$$\langle \Delta \bar{R}_{\|} \rangle(t) \simeq -18^{1/3}\left(\frac{Lt}{\hat{\zeta}\ell_p^2}\right)^{1/3} \quad \text{(release)} \tag{100}$$

follows from Eq. (91b). We expect the growth law $\langle \Delta \bar{R}_{\|} \rangle \propto t^{1/3}$ during homogeneous tension relaxation to hold even for chains with $L \gg \ell_p$. The example of retracting DNA will be discussed as an experimental outlook in Sec. VI. The exponent 1/3 coincides with that obtained by an adiabatic application of the stationary force-extension relation [16] to a "frictionless" [17] polymer with attached beads at its ends [18].

For times $t \gg t_\star = L^8/\ell_p^4$ the growth law in Eq. (100) crosses over to the one noted in Table III. Interestingly, both growth laws appearing for $t \gg t_L^{\|}$ are independent of the initial tension $\mathfrak{f}$. In both cases, the initial conditions are completely "forgotten" once the tension has propagated through the whole polymer. An overview over the time scales separating the diverse regimes for release (as compared to pulling) will be given in Sec. V F.

TABLE III. Universal bulk contribution $\langle \Delta \bar{R}_{\|} \rangle(t)$ to the dynamic change of the end-to-end distance in the limit $t_\star \ll t \ll t_L^{\perp}$.

Problem	$t \ll t_{\mathfrak{f}}$	$t \gg t_{\mathfrak{f}}$
Pulling	$[L\mathfrak{f}/\ell_p\Gamma(7/4)](t/2)^{3/4}$ [14,15]	$(L/\ell_p)\sqrt{2\mathfrak{f}t/\pi}$
Release	$-[L\mathfrak{f}/\ell_p\Gamma(7/4)](t/2)^{3/4}$	$[-2^{3/4}/\Gamma(1/4)](L/\ell_p)t^{1/4}$

D. Pulling and release for small forces

Provided the external force is smaller than the critical Euler buckling force of the polymer, $\mathfrak{f} < L^{-2}$, the crossover time $t_{\mathfrak{f}}$ exceeds the terminal relaxation time $t_L^{\perp}$; hence, the linearized PIDE (32), applies throughout the contour relaxation. The linearity allows to solve the PIDE for a polymer of finite length, and we obtain an analytic description of the crossover between the asymptotic power laws $\Delta \bar{R}_{\|}(t) \propto t^{7/8}$ for $t \ll t_L^{\|}$ and $\Delta \bar{R}_{\|}(t) \propto t^{3/4}$ for $t_\star \ll t \ll t_L^{\perp}$ (cf. Tables II and III). To this end, let us first reinstall original units (which are better adapted for the present purpose) into the linearized PIDE (32),

$$\partial_s^2 F(s,z) = \frac{z^{1/4}\hat{\zeta}}{2^{3/4}\ell_p} F(s,z), \tag{101}$$

where $F(s,z)$ is the Laplace transformation of the integrated tension,

$$F(s,z) \equiv \int_0^\infty dt e^{-zt} F(s,t). \tag{102}$$

For the boundary conditions of pulling, Eqs. (15) and (16a), the solution to Eq. (101) is given by

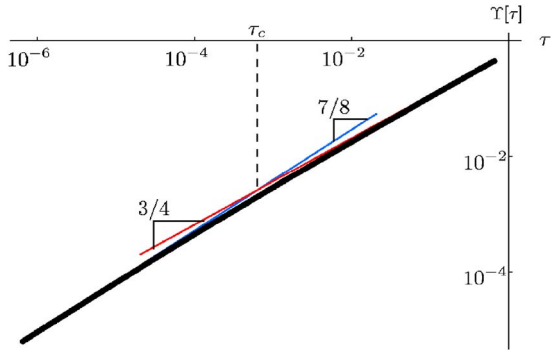

FIG. 5. (Color online) The scaling function $\Upsilon(\tau)$ in a double-logarithmic plot. The crossover of the scaling behavior is close to the time $\tau_c=6.55\times10^{-4}$ where the asymptotic short- (blue) and long- (red) time asymptotics cross.

$$F(s,z)=\mathfrak{f}z^{-2}\frac{\cosh[(\hat{\zeta}/\ell_p)^{1/2}(z/8)^{1/8}(s-L/2)]}{\cosh[(\hat{\zeta}/\ell_p)^{1/2}(z/8)^{1/8}L/2]}. \quad (103)$$

This implies a growth of the end-to-end distance of

$$\langle\Delta\bar{R}_\parallel\rangle(z)=-2\hat{\zeta}^{-1}\partial_s F|_{s=0}=\frac{2^{5/8}\mathfrak{f}}{z^{15/8}(\hat{\zeta}\ell_p)^{1/2}}\tanh\left[\left(\frac{\hat{\zeta}}{\ell_p}\right)^{1/2}\left(\frac{z}{8}\right)^{1/8}\frac{L}{2}\right]. \quad (104)$$

The Laplace back-transform of Eq. (105) takes the form

$$\langle\Delta\bar{R}_\parallel\rangle(t)=\int_{-i\infty+\epsilon}^{i\infty+\epsilon}\frac{dz}{2\pi i}e^{zt}\langle\Delta\bar{R}_\parallel\rangle(t)=\frac{\mathfrak{f}\hat{\zeta}^3L^7}{\ell_p^4}\Upsilon\left[\left(\frac{t}{L^4}\right)\left(\frac{\ell_p}{\hat{\zeta}L}\right)^4\right], \quad (105)$$

where $\Upsilon(\tau)$ is a scaling function, given by

$$\Upsilon(\tau)=\frac{2^{5/8}}{\pi}\int_0^\infty ds\frac{e^{-x\tau}-1}{x^{15/8}}\mathrm{Im}[e^{-i(7/8)\pi}\tanh(2^{-11/8}x^{1/8}e^{i\pi/8})]. \quad (106)$$

We have depicted $\Upsilon(\tau)$ in a double-logarithmic plot in Fig. 5 together with the corresponding asymptotics from Tables II and III. Note that the time $\tau_c\approx6.55\times10^{-4}$ where the asymptotic lines cross is a good indication of the crossover occurring in the exact solution. Assuming that this also holds quite generally, it is possible to obtain estimations of when the crossover between linear and nonlinear regimes should occur in the natural time units $t_\mathfrak{f}$. To this end, one simply equates the corresponding asymptotic power laws (including the exact prefactors) for the growth of the end-to-end distance. As for the present case with $\tau_c\approx6.55\times10^{-4}$, these crossover times are typically not of order 1 in natural units because of the numerical proximity of the exponents of the asymptotic power laws, which are 7/8 and 3/4 in the present case. In a given experimental situation, one should therefore check carefully which regime is expected by comparing experimental time scales with these unusual crossover times.

E. FDT and linear response

According to the fluctuation-dissipation theorem (FDT [19,20]), the fluctuations in the end-to-end distance should be related to the linear response of the polymer. It is tempting to interpret the linear short-time regime, where $\langle\Delta\bar{R}\rangle\simeq\mathfrak{f}t^{7/8}(\hat{\zeta}\ell_p)^{-1/2}$, as linear response in the usual sense, in which case the fluctuations of the end-to-end distance should, according to the FDT, scale as $\langle\Delta\bar{R}^2\rangle\simeq t^{7/8}\hat{\zeta}^{-1/2}\ell_p^{-3/2}$ in equilibrium. However, fluctuations of this strength are inconsistent with a deterministic tension dynamics, because they generate friction forces over a scale $\ell_\parallel(t)\simeq t^{7/8}(\ell_p/\hat{\zeta})^{1/2}$ and thus imply tension fluctuations of magnitude

$$\delta f\simeq\hat{\zeta}\ell_\parallel(t)\langle\Delta\bar{R}\rangle/t\simeq(\zeta/\ell_p)^{1/4}t^{-7/16}. \quad (107)$$

Tension fluctuations exceed the applied force in magnitude at any given time for small enough external forces. Hence, in the limit $\mathfrak{f}\to0$ while $\epsilon\ll1$ is fixed, the tension cannot be considered as a deterministic quantity. Recall, however, that our MSPT analysis in part I was based on the limit $\epsilon\to0$ while $\mathfrak{f}$ is fixed, and only in this limit does the self-averaging argument of part I apply. Extending our results to the usual linear response limit corresponds to the uncontrolled approximation $fr_\perp'^2\to f\langle r_\perp'^2\rangle$. To analyze this limit more carefully, one has to solve the stochastic PIDE obtained in part I before the self-averaging argument was employed. However, since the 7/8 scaling of the fluctuations has already been confirmed in simulations [10], we expect that such a more rigorous analysis would yield the same scaling but a prefactor different from the one of the deterministic short-time law (Table II).

F. Release versus pulling (overview)

The diverse regimes and their range of validity are summarized in Fig. 6 for the pulling and the complementary release problem. It depicts the crossover time scales as a function of the externally applied tension $\mathfrak{f}$. The line $t_\mathfrak{f}\simeq\mathfrak{f}^{-2}$ separates "linear" from "nonlinear" behavior. The symmetry of the graph for $t<t_\mathfrak{f}$ with respect to the $\mathfrak{f}=0$ axis indicates that the scenario of pulling can indeed be considered as the inverse scenario of release for weak forces $f\ll f_c$, or, more generally, at short times. This symmetry is lost in the nonlinear regime. The growing importance of uniform tension relaxation for release with increasing initial tension $\mathfrak{f}$ becomes particularly apparent on the logarithmic scale of the figure. Due to the particular choice of units (t/L^4 and f/L^{-2}), the regimes of nonlinear growth of the boundary layers appear relatively narrow in Fig. 6. Which of the various regimes will pre-dominantly be observed in measurements actually depends strongly on the ratio L/ℓ_p and on the experimentally accessible time scales.

G. Towing

Towing was excluded from the preceeding discussion because it is the only "asymmetric" problem, as both ends of the polymer behave differently. In the tension propagation

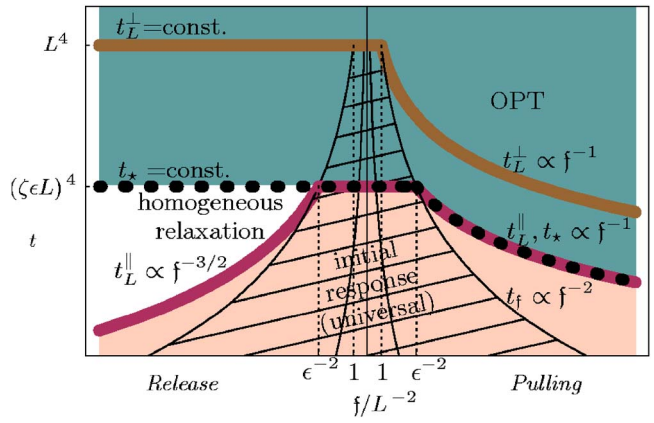

FIG. 6. (Color online) Characteristic times (logarithmic scale) for pulling and release against the applied external force $\mathfrak{f}$ (linear scale). The time $t_\star$ (stars) separates regions where ordinary perturbation theory (OPT) applies (dark shaded) from regions (light shaded) of linear (hatched) and nonlinear tension propagation and from homogeneous tension relaxation (white). Whereas longitudinal friction is negligible for $t > t_\star$, it limits the dynamics for $t < t_\star$. The innermost funnel-shaped region indicates the regime where the tension fluctuations are important [defined by $f < \delta f$ with δf given by Eq. (107)].

regime ($t \ll t_L^\parallel$), the left end is constrained to move with constant velocity, while the right end experiences no driving force. Hence, we have

$$\langle \Delta \bar{R}_\parallel \rangle(t) = vt, \quad \text{for } t \ll t_L^\parallel. \tag{108}$$

After the boundary layer of nonzero tension has reached the free end, $t \gg t_L^\parallel$, the right end starts to move. Then, the tension profile becomes linear as for a straight rod dragged through a viscous solvent. The further contour relaxation is up to prefactors identical to the pulling problem for $t \gg t_L^\parallel \approx t_\star$.

H. Pushing

For completeness, we mention the scenario of a filament being compressed by external longitudinal forces. This scenario has some subtleties. Pushing increases the stored length exponentially for $t \gg t_\mathfrak{f}$ by virtue of the Euler buckling instability and generates a situation where the weakly bending approximation is not valid anymore. Then, hairpins are generated [21] and for $t \gg t_f$ the rigidly oriented driving forces *pull* on those hair pins. Our theory is only applicable at short times. For $t \ll t_f$ the response of the system is linear in the driving force, irrespective of the sign.

I. Boundary effects

Up to now, we only discussed the change $\langle \Delta \bar{R}_\parallel \rangle(t)$ in projected end-to-end distance corresponding to the change $\langle \Delta \bar{\varrho} \rangle$ of the stored length in the bulk. For a hinged and clamped semi-infinite polymer, respectively, the as-yet missing boundary contribution $X^{h/c}(t) \equiv \langle \Delta R_\parallel^{h/c} \rangle - \langle \Delta \bar{R}_\parallel \rangle$ is given by

TABLE IV. Boundary contribution to the change $\langle \Delta R_\parallel^{h/c} \rangle(t)$ of the end-to-end distance for hinged and clamped ends, respectively, in the limit $t_L^\perp \ll t$.

Problem	$\langle \Delta R_\parallel^{h/c} \rangle(t) - \langle \Delta \bar{R}_\parallel \rangle(t)$
Pulling	$\pm 2t\mathfrak{f}/\ell_p$
Towing	$\pm 2t\mathfrak{f}/\ell_p$
Release	$\begin{cases} \pm 2t\mathfrak{f}/\ell_p, & \text{for } f_< \ll L^{-2} \\ 0, & \text{for } f_< \gg L^{-2} \end{cases}$

$$X^{h/c}(t) = \pm 2 \int_0^\infty ds \int_0^\infty \frac{dq}{\pi \ell_p} \left\{ \frac{e^{-2q^2[q^2 t + F(s,t)]} - 1}{q^2 + f_<} + 2q^2 \int_0^t d\tilde{t} e^{-2q^2[q^2(t-\tilde{t}) + F(s,t) - F(s,\tilde{t})]} \right\} \cos(2qs). \tag{109}$$

As discussed in part I, the boundary-dependent term of the stored length decays on a length scale of $O(1)$ due to the cosine factor. Since the tension decays on a much larger length scale of order $O(\epsilon^{-1/2})$, it is permissible to use the (integrated) tension at $s=0$ to evaluate the arclength integral in Eq. (109).

Upon replacing $F(s,t) \to F(0,t)$ and using

$$\int_0^\infty ds \cos(2qs) = (\pi/2)\delta(q),$$

the integral in Eq. (109) can be evaluated,

$$X^{h/c}(t) = \pm \lim_{q \to 0} \frac{2}{\ell_p} \frac{q^2[q^2 t + F(0,t)]}{q^2 + f_<}, \tag{110}$$

which vanishes, unless

$$f_< = 0 \Rightarrow X^{h/c}(t) = \pm \frac{2F(0,t)}{\ell_p}. \tag{111}$$

In the semi-infinite arclength interval, these boundary contributions are therefore nonzero only for pulling and towing, and are summarized in Table IV. Note that the boundary effects of clamped (hinged) ends tend to reduce (increase) the longitudinal response of the polymer in comparison to the bulk response. This may be explained as follows. Close to a clamped end, a polymer is more stretched out than in the bulk because $\boldsymbol{r}_\perp'^{\,2}$ is constrained to approach zero at the end. As a consequence, the end portion of the polymer is less able to store or release excess length. For hinged ends, the boundary conditions act just in the reverse direction.

The strict vanishing of the boundary term for any finite $f_<$ and the discontinuity at $f_<=0$ is a consequence of the assumed infinite half-space. For a polymer of finite length, it turns out that the boundary term approaches zero for prestretching forces larger than the critical Euler buckling force, $f_< \gg f_c \equiv L^{-2}$. This can be seen by studying the finite integral $\int_0^L ds[\langle \Delta \varrho^{h/c} \rangle(s,t) - \langle \Delta \bar{\varrho} \rangle(s,t)]$. For forces $f_< \ll f_c$, the integrand saturates at a plateau of magnitude $O(f_<^{3/2} t/\ell_p)$ for

$\ell_\perp(t) < s < f_<^{-1/2}$ before it finally decays to zero. Within the semi-infinite integral, the integral over this long plateau cancels the contribution stemming from $s < \ell_\perp(t)$, as required by Eq. (110). However, for $L \ll f_<^{-1/2}$ the contribution from the plateau may be neglected. As a consequence, the value of the integral is for $f_< \ll f_c$ given by $\pm 2 f_< t/\ell_p$. This asymptotic behavior is important for release, as noted in Table IV.

Upon comparing Table IV with Tables II and III, one may think that boundary effects are always subdominant in the short-time limit. However, our calculations were specialized to hinged or clamped boundary conditions. In many experimental situations, one has to deal with *free* boundary conditions. Somewhat tedious but rigorously, these boundary conditions can be taken into account by means of the correct susceptibility, which can only be given in terms of an integral. Here, we discuss effects related to free boundary conditions on a heuristic basis and show that they generate a *dominant* contribution to the change in the end-to-end distance for pulling, which is proportional to $t^{3/4}$.

The argument is based on the observation that external forces that act in the longitudinal direction ($\parallel$) while the polymer is free automatically introduce small [of order $O(\epsilon^{1/2})$] transverse forces at the ends. This follows from the force balance equation of a semiflexible polymer (cf. part I),

$$\kappa \boldsymbol{r}''' + \boldsymbol{f}_{\mathrm{el}} = f \boldsymbol{r}', \tag{112}$$

where $\boldsymbol{f}_{\mathrm{el}}(s)$ is the elastic force acting at arclength s. At the ends, where $\boldsymbol{f}_{\mathrm{el}}$ points in the longitudinal direction to cancel the external pulling force, one obtains from the projection of Eq. (112) onto the transverse axis

$$\boldsymbol{r}'''_\perp = f \boldsymbol{r}'_\perp = \mathfrak{f} \boldsymbol{r}'_\perp + O(\epsilon) \quad \text{(at the ends)}. \tag{113}$$

Thus, $\boldsymbol{r}'''_\perp$ is typically nonzero at the ends because the slope $\boldsymbol{r}' = O(\epsilon^{1/2})$ fluctuates. This, however, corresponds to a transverse force at the end, which results in a transverse deformation. The corresponding bulge of contour is only visible on the microscale because it spreads with the transverse correlation length $\ell_\perp(t) \simeq t^{1/4}$. Nevertheless, this deformation may dominate the growth of the end-to-end distance, as is demonstrated for pulling: With the transverse bulk susceptibility scaling as $\bar{\chi}(t) \simeq t^{-1/4}$ we estimate the magnitude of transverse deformation $\Delta r_\perp(s=0,t) \equiv r_\perp(0,t) - r_\perp(0,0)$ induced by a transverse force of magnitude $\mathrm{ord}(\mathfrak{f}\epsilon^{1/2})$ by

$$\mathrm{ord}(\langle |\Delta r_\perp(0,t)| \rangle) \simeq \mathfrak{f}\epsilon^{1/2} t \bar{\chi}(t) \simeq \epsilon^{1/2} t^{3/4} \mathfrak{f}. \tag{114}$$

The displacement of the end couples to the projected length because of the mismatch of the end tangent with the $\parallel$ axis by a small angle of typical magnitude $\langle |r'_\perp(s=0)| \rangle \simeq \mathrm{ord}(\epsilon^{1/2})$. The expected growth of the end-to-end distance due to this effect is therefore estimated by

$$\langle \Delta R_\parallel^{h/c} \rangle(t) - \langle \Delta \bar{R}_\parallel \rangle(t) \simeq \langle |r'_\perp(s=0)| \rangle \langle |\Delta r_\perp(0,t)| \rangle \simeq \epsilon t^{3/4} \mathfrak{f} = \frac{L}{\ell_p} t^{3/4} \mathfrak{f}. \tag{115}$$

This dominates over the growth law of the bulk, which scales like $t^{7/8}/\sqrt{\ell_p}$ at short times. The only way to avoid the outlined effect is to apply the external force strictly tangentially to the end tangents, which is, however, somewhat unrealistic. The same problem will experimentally arise in the short-time limit of release if the prestretching force was not applied strictly tangentially. However, the long-time limits are unaffected by this subtlety because the bulk contributions dominate over contributions from the end.

To our knowledge, these end effects have so far masked the subdominant $t^{7/8}$ contribution in experiments that monitored the time-dependent end-to-end distance (we note that in Ref. [22] the 7/8 scaling is inferred from a corresponding scaling of the measured shear modulus of an active gel). As we outline in Sec. VI B, force spectroscopy, on the contrary, may allow one to measure the tension dynamics, which is itself truly *independent* of the boundary conditions imposed on the transverse displacements.

VI. SUGGESTIONS FOR EXPERIMENTS

While many experiments have been done concerning flexible polymers in external force fields [23,24], the available measurements on driven stiff or prestretched polymers is not sufficient to verify our predictions. Most of these experiments have monitored the transverse and longitudinal response at intermediate times where OPT is valid (e.g., [25]). Investigations concerning the longitudinal short-time dynamics are scarce [17,22,26]. In the following, we propose several assays that might be able to fill this gap.

To facilitate the application of our predictions, we reintroduce the parameters κ and ζ for the following.

A. Strongly stretched DNA

The experimental verification of most of our results requires stiff polymers with a total length much smaller than their persistence length. A remarkable exception is release in the regime of homogeneous tension relaxation, which was discussed in Sec. IV. For polymers with $L \gg \ell_p$, like a typical DNA molecule, this regime appears if the prestretching force obeys

$$\mathfrak{f} \gg \mathfrak{f}_{\ell_p} \equiv \kappa \ell_p^{-2} = \frac{k_B T}{\ell_p}, \tag{116}$$

where $\mathfrak{f}_{\ell_p}$ is the Euler buckling force corresponding to the buckling length ℓ_p. For forces much larger than the crossover force $\mathfrak{f}_{\ell_p}$, the polymer may be considered as weakly bending. For those long, but strongly stretched polymers our analysis of release predicts the following.

After the stretching force has been released the tension first propagates through the filament. This regime [12,18] ends at the time

$$t_L^{\parallel} = \frac{\zeta_\parallel L^2 \ell_p}{k_b T} \left(\frac{\mathfrak{f}}{\mathfrak{f}_{\ell_p}} \right)^{-3/2} \equiv \tau_R \left(\frac{\mathfrak{f}}{\mathfrak{f}_{\ell_p}} \right)^{-3/2} \tag{117}$$

when the tension has to propagated through the filament. Here, $\tau_R \equiv \zeta_\parallel L^2 \ell_p/(k_B T)$ scales like the longest relaxation time of a Rouse chain with segment length ℓ_p. The characteristic time $t_L^{\parallel} \ll \tau_R$ marks the crossover to a regime where

the tension profile is roughly parabolic and slowly decays according to the power law $f(t) \propto t^{-2/3}$. This is associated with the projected length $R_\parallel$ growing like

$$\langle \Delta R_\parallel(t) \rangle \equiv \langle R_\parallel(t) - R_\parallel(0) \rangle = 18^{1/3} L \left(\frac{t}{\tau_R} \right)^{1/3}. \quad (118)$$

The above analysis strictly holds for the portion of the polymer that stays weakly bending. This is not the case at the boundaries, for which we refer to existing theories. According to the stem-flower model of Refs. [27–29] the boundaries will develop in time t a "flower" of arclength

$$\ell_{\text{flower}}(t) \simeq L \left(\frac{t}{\tau_R} \right)^{1/2}, \quad (119)$$

thereby reducing the end-to-end distance by an amount of the same order of magnitude as ℓ_{flower} itself. It is seen that for $t \ll \tau_R$ the shrinkage of the end-to-end distance due to the flower is much smaller than that due to the weakly bending part of the polymer (the stem), Eq. (118).

Thus, the evolution of the end-to-end distance should be described by Eq. (118) even for flexible polymers if the prestretching force is large enough. Since DNA can be stretched by very large forces without unzipping or destroying the covalent bonds, we think that the scaling $\langle \Delta R(t) \rangle \propto t^{1/3}$ should be visible in a release experiment with DNA. The relevant quantities in an experiment with λ-phage DNA (as in Ref. [26]) in aqueous solution would be

$$\ell_p \approx 50 \text{ nm}, \quad L \approx 20 \ \mu\text{m},$$

$$a \approx 2 \ \mu\text{m} \quad \text{(thickness)},$$

$$\zeta_\perp \approx 4\pi\eta/\ln(L/a) \approx 1.3 \times 10^{-3} \text{ Pa s},$$

$$\mathfrak{f}_{\ell_p} \approx 0.08 \text{ pN}, \quad \tau_R \approx 7 \text{ s}. \quad (120)$$

Though it might require extreme conditions to reach the asymptotic limit in Eq. (118), any experiment with finite prestretching forces larger than f_c should be suitable for deciding the question whether or not the stem dominates the retraction. One would then compare the data with a numerical solution [30] of the governing equation (1), which describes the stress relaxation in stiff wormlike chains.

B. Single-molecule force spectroscopy

1. Towing

As we already mentioned in Sec. III C, towing offers the possibility to measure the tension propagation by a force measurement. The experimental idea is illustrated in Fig. 7(a). The polymer's left end is suddenly pulled, e.g., by an optical tweezer whose focus moves with constant velocity. As a consequence the pulled end follows the laser beam with (almost[4]) constant velocity. By measuring the deflection of the trapped end from the center of the beam one can, in principle, extract the pulling force $\mathfrak{f}(t)$ and thus the size $\ell_\parallel(t) \simeq \mathfrak{f}(t)/(\hat{\zeta} v)$ of the boundary layer. However, since the laser beam is moving, it might represent some problems to dynamically extract the deflection.

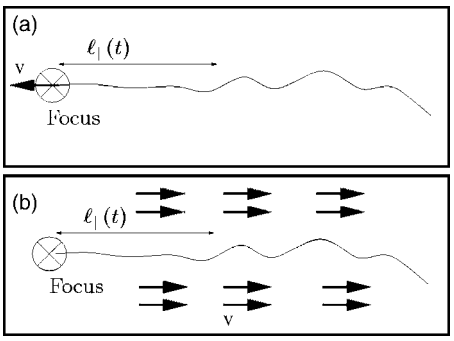

FIG. 7. Two possible realizations of towing. In (a) the polymer's left end is being dragged through the solvent with constant velocity $\boldsymbol{v}$, whereas in (b) the optical tweezer is immobile while the solvent flows with constant velocity $\boldsymbol{v}$. In both experiments, the length $\ell_\parallel(t)$ of the boundary layer is derived from the pulling force of the tweezer, which can be inferred from the displacement of the end within the focus of the tweezer.

A solution to the latter problem is suggested by the following Gedanken experiment. Consider the above realization of towing in the coordinate frame comoving with the left tip, as illustrated in Fig. 7(b). Then, it seems as if the bulk of the polymer was dragged by a homogeneous force field to the right while the left end is held fixed by the optical tweezer, just as if the optical tweezer was spatially fixed while the solvent was homogeneously flowing to the right. In fact, from the polymer's perspective there is no difference between both experiments. Thus, we propose to graft one end of a polymer by a tweezer or by the cantilever of an atomic force microscope. Then, a homogeneous force field (electric field or fluid flow) is suddenly turned on that pulls the bulk of the polymer to the right. The deflection of the tip gives the pulling force and hence the length of the boundary layer.

2. Onset of the nonlinear regime

One would like to estimate typical time sales for the diverse regimes of tension propagation and relaxation. As we have seen above, most of the time scales crucially depend on the total length of the polymer—e.g., $\ell_\parallel(t) \propto L^8$ in the linear regime. This high tunability is of experimental advantage because one can adjust the setup to the observable time scales. On the other hand, it forbids one to give *typical* time scales for those quantities.

However, there are characteristic quantities that do not depend on the length of the polymer. Probably the most interesting one is the threshold to the nonlinear regime: when the product of driving force and the square root of the applied time exceed a certain value I_c the polymer response becomes nonlinear,

[4]Due to the finite stiffness of the harmonic laser potential, the trapped end will not be moved with *exactly* the same velocity as the trap during a transient, in which the end approaches its steady-state location within the laser potential.

TABLE V. Threshold values $I_c=\sqrt{\kappa\zeta_\perp}$ for diverse biopolymers.

Polymer	I_c
Microtubuli	1.6×10^2 pN ms$^{1/2}$
F-actin	10 pN ms$^{1/2}$
Intermediate fil.s	4 pN ms$^{1/2}$
DNA	0.9 pN ms$^{1/2}$

$$\text{f}\sqrt{t} \gg I_c \equiv \sqrt{\kappa\zeta_\perp} = \sqrt{k_B T \ell_p \zeta_\perp}. \tag{121}$$

With persistence lengths of ℓ_p=7 mm, 17 μm, 2 μm, and 50 nm for microtubuli [31,32], F-actin [25], intermediate filaments, and DNA [16], respectively, and corresponding friction coefficients $\zeta_\perp \approx 4\pi\eta/\ln(\ell_p/a)$ (transverse friction coefficient per length of a rod of length ℓ_p), we have evaluated I_c for some common biopolymers; see Table V. Those values can be used to decide whether the response of a given biopolymer under a "typical" time-dependent external longitudinal force is predominantly nonlinear or linear. During a power stroke, for instance, the molecular motor myosin exerts a force of about 5 pN on an actin filament during a time of roughly 1 ms (cycle time of the power stroke). Hence, the impulse of about $0.5I_c$ is somewhat smaller than I_c for actin, so that the actin response should be linear.

VII. SUMMARY AND OUTLOOK

In this paper, we have studied the tension dynamics of a weakly bending semiflexible polymer in a viscous fluid theoretically. Starting from the coarse-grained equation of motion for the tension, Eq. (4), we elaborated the nonlinear longitudinal dynamic response to various external perturbations (mechanical excitations, hydrodynamic flows, electrical fields, etc.) that can be represented as sudden changes of boundary conditions. For the various scenarios we identified two-parameter scaling forms that capture the crossover from linear to nonlinear tension dynamics. In the limit of large and small arguments, where the equilibrium structure of the polymer is self-affine, they were shown to reduce to one-parameter scaling forms, which could be calculated analytically in most cases. The growth law $\ell_\parallel(t)\sim t^\zeta$ of the tension profiles could be inferred from the scaling variables of the respective scenarios. This enabled us to develop a unified theory of tension propagation. Not only does it contain all cases (correctly) studied in the literature so far. It also identifies their ranges of validity and provides new predictions. The recovered known results and our new predictions are summarized in Figs. 3 and 6 and Tables I–III.

Various dynamic regimes should be well realizable for certain biopolymers. A novel regime of homogeneous tension relaxation is a particularly remarkable result from the experimental point of view (Sec. VI A). In contrast to previous expectations, this regime is predicted to dominate the relaxation of strongly stretched DNA. Moreover, it is an intriguing question whether the tension propagation laws $\ell_\parallel(t)$ govern mechanical signal transduction through the cytoskeleton [33,34]. We expect that the force spectroscopical methods, proposed in Sec. VI B, might be helpful to answer these questions.

Inclusion of hydrodynamic interactions merely produces logarithmic corrections but would give rise to more interesting effects for polymerized membranes to which our discussion could be generalized with otherwise little change. Other natural generalizations including the transverse nonlinear response of polymers [8], quenches in the persistence length [13], and more complex force protocols [35] are currently also under investigation. An experimentally important scenario is a stiff polymer in a shear flow, which was studied in Ref. [36] with the approximation of a space-independent tension. Extending this work to include tension dynamics is desireable but somewhat involved: The shear flow randomly triggers a characteristic mixture of rotational and bending motion of the polymer. The external force profile during these "tumbling" events depends on the random contour undulations of the polymer. These random fluctuations determine how the flow-induced forces are distributed along the polymer. Therefore, the pattern of tension dynamics will not be deterministic, as in the scenarios considered in the present contribution, but stochastic. With the need to develop new analytical methods and simulations to deal with such fluctuating tension profiles, the problem of a polymer in shear flow points towards a challenging future research direction in this field.

ACKNOWLEDGMENTS

It is a pleasure to acknowledge helpful conversations with Benedikt Obermayer, who, in addition, corrected several prefactors. This research was supported by the German Academic Exchange Service (DAAD) through a grant within the Postdoc-Program (OH) and by the Deutsche Forschungsgemeinschaft through Grants Nos. Ha 5163/1 (O.H.) and SFB 486 (E.F.).

APPENDIX A: CROSSOVER SCALING (DETAILS)

1. Deterministic relaxation at long times ($t \gg t_\text{f}$)

We have for $c=0$

$$A - \int_{-\infty}^{\infty} \frac{dq}{2\pi}\frac{1}{q^2}(1-e^{-2q^2\phi}) = \sqrt{\phi}\int_{-\infty}^{\infty}\frac{dq}{2\pi}\frac{1}{q^2}(e^{-2q^2}-e^{-2q^2(q^2\tau\phi^{-2}+1)}) \overset{\tau\gg1}{\to} 0, \quad \text{if } \phi^{-2}=o(\tau^{-1}), \tag{A1}$$

and for $c=1$

$$A - \int_{-\infty}^{\infty}\frac{dq}{2\pi}\frac{1}{q^2+1} = -\int_{-\infty}^{\infty}\frac{dq}{2\pi}\frac{1}{q^2+1}e^{-2q^2(q^2\tau+\phi)} \overset{\tau\gg1}{\to} 0, \quad \text{if } \phi^{-2}=o(\tau^{-1}). \tag{A2}$$

As indicated, both expressions, Eqs. (A1) and (A2), go to zero for large τ if $\phi^{-2}=o(\tau^{-1})$. The latter, however, follows

from the assumptions stated in the main text: namely, that the tension satisfies the scaling form, Eq. (28), with the requirement in Eq. (27). N.B. It turns out that $\phi = O(\tau)$ for pulling and release and $\phi = O(\tau^{4/3})$ for towing.

2. Thermal excitation at long times ($t \gg t_f$)

We want to show that it is justified to calculate (the negative of) the thermally generated stored length represented by the term B, Eq. (47b), at long times *quasistatically* for the semi-infinite polymer. To this end, we first insert the scaling ansatz, Eq. (28), for $\phi(\sigma,\tau)$,

$$B = -4\int_{\Lambda^{-1}}^{\infty}\frac{dq}{2\pi}q^2\int_0^{\tau}d\hat{\tau} \times e^{-2q^2(q^2(\tau-\hat{\tau})+\tau^{\alpha+1}\{\hat{\phi}(\xi)-(\hat{\tau}/\tau)^{\alpha+1}\hat{\phi}[\xi(\tau/\hat{\tau})^z]\})}, \quad \text{(A3)}$$

where we introduced the scaling variable $\xi \equiv \sigma/\tau^z$. Then we substitute $\hat{\tau} \to x\tau$ and $q \to q\tau^{-1/4}$,

$$B = -4\tau^{1/4}\int_{\Lambda^{-1}\tau^{1/4}}^{\infty}\frac{dq}{2\pi}q^2\int_0^1 dx \times e^{-2q^2\{q^2(1-x)+\tau^{\alpha+1/2}[\hat{\phi}(\xi)-x^{\alpha+1}\hat{\phi}(\xi x^{-z})]\}}. \quad \text{(A4)}$$

Note that for $\alpha > -1/2$ [as assumed in Eq. (27)] the factor $\tau^{\alpha+1/2}$ in the exponent diverges in the long-time limit. Hence, for any given wave number the x integral will be dominated by x close to 1 for large enough $\tau \gg 1$. This allows us to linearize the exponent in $1-x$ when performing the x integral for this given wave number. In contrast, for a given time τ and $\hat{\phi}(\xi) = O(1)$, the exponent can be linearized only for large enough wave numbers, $q \gg q_\star(\tau) \equiv \tau^{-\alpha/2-1/4}$, for which the factor $q^2\tau^{\alpha+1/2} \gg 1$ in the exponent of Eq. (A4) is much larger than 1.

Since the integral over q runs over all q vectors, we have also to care about the small wave numbers, for which the exponent cannot be linearized in $1-x$. To this end, we split the q integral at a wave vector K satisfying

$$q_\star^{1/3} \gg K \gg q_\star \equiv \tau^{-\alpha/2-1/4}, \quad \text{(A5)}$$

which can be found in the limit $\tau \gg 1$ under the premise of Eq. (27), $\alpha > -1/2$. The first inequality in Eq. (A5) is required for reasons that become clear later on. For the upper part $B_>$ of the integral we can linearize the exponent in $1-x$,

$$\begin{aligned} B_> &\equiv -4\tau^{1/4}\int_K^{\infty}\frac{dq}{2\pi}q^2\int_0^1 dx \times e^{-2q^2\{q^2(1-x)+\tau^{\alpha+1/2}[\hat{\phi}(\xi)-x^{\alpha+1}\hat{\phi}(\xi x^{-z})]\}} \\ &\sim -4\tau^{1/4}\int_K^{\infty}\frac{dq}{2\pi}q^2\int_0^1 dx e^{-2q^2(1-x)[q^2+\tau^{1/2}\partial_\tau(\tau^{\alpha+1}\hat{\phi}(\sigma/\tau^z))]} \\ &= -2\tau^{1/4}\int_K^{\infty}\frac{dq}{2\pi}\frac{1-e^{-2q^2[q^2+\tau^{1/2}\partial_\tau(\tau^{\alpha+1}\hat{\phi}(\sigma/\tau^z))]}}{q^2+\tau^{1/2}\partial_\tau(\tau^{\alpha+1}\hat{\phi}(\sigma/\tau^z))}, \end{aligned} \quad \text{(A6)}$$

where we eliminated the scaling variable $\xi = \sigma/\tau^z$, again. Using the second inequality in Eq. (A5) it is seen that we can drop the exponential for the "interesting" regime $\hat{\phi}(\sigma/\tau^z) = O(1)$, where the tension has an appreciable value. Inserting back $\phi = \tau^{\alpha+1}\hat{\phi}(\sigma,\tau)$ we obtain

$$\begin{aligned} B_> &\sim -2\tau^{1/4}\int_K^{\infty}\frac{dq}{2\pi}\frac{1}{q^2+\tau^{1/2}\partial_\tau\phi(\sigma,\tau)} \\ &= \frac{2}{\sqrt{\partial_\tau\phi(\sigma,\tau)}}\int_{K/[\tau^{1/4}\sqrt{\partial_\tau\phi(\sigma,\tau)}]}^{\infty}\frac{dq}{2\pi}\frac{1}{q^2+1} \sim -\frac{1}{2\sqrt{\partial_\tau\phi(\sigma,\tau)}}. \end{aligned} \quad \text{(A7)}$$

To obtain the last asymptotics, we have approximated the lower bound of the integral by zero. This can be justified by the first inequality in Eq. (A5),

$$\frac{K}{\tau^{1/4}\sqrt{\partial_\tau\phi(\sigma,\tau)}} = KO(\tau^{-1/4-\alpha/2} = q_\star) \ll q_\star^{4/3} \ll 1.$$

The remaining lower part $B_<$ of the q integral in Eq. (A4) is estimated to be small as compared to $B_>$,

$$\begin{aligned} B_< &\equiv -4\tau^{1/4}\int_{\Lambda^{-1}t^{1/4}}^{K}\frac{dq}{2\pi}q^2\int_0^1 dx \times e^{-2q^2\{q^2(1-x)+\tau^{\alpha+1/2}[\hat{\phi}(\xi)-x^{\alpha+1}\hat{\phi}(\xi x^{-z})]\}} \\ &< -4\tau^{1/4}\int_0^{K}\frac{dq}{2\pi}q^2\int_0^1 dx \\ &= -\frac{4}{3}\tau^{1/4}K^3/(2\pi) \ll -\frac{4}{3}\tau^{-\alpha/2}/(2\pi) \propto B_>, \end{aligned} \quad \text{(A8)}$$

where the first inequality in Eq. (A5) has been applied. Therefore, B is asymptotically given by Eq. (A7).

APPENDIX B: RELAXATION OF A COMPLETELY STRETCHED POLYMER

In this section, we consider more closely the intermediate asymptotics

$$f \propto \left(\frac{\hat{\zeta}L^2}{l_p t}\right)^{2/3}, \quad \text{(B1)}$$

which is approached in the limit

$$t_L^{\parallel} = \frac{\hat{\zeta}L^2}{l_p f_<^{3/2}} \ll t \ll t_\star = \frac{\hat{\zeta}^4 L^8}{l_p^4} \quad \text{(B2)}$$

of release, which we analyzed in terms of a quasistatic approximation in Sec. V B. The purpose of this section is to justify the quasistatic assumption in the limit of $f_< \to \infty$ (i.e., $t_f \to 0$) where we start with a completely stretched polymer and all stored length is generated by the action of stochastic forces.

To this end, we show that, in the limit $t \to 0$, the change in stored length $\langle \Delta\bar{\varrho} \rangle$ given by Eq. (3) for the force history given by Eq. (B1) asymptotically approaches the value one obtains from the quasistatic calculation,

$$\langle \Delta\bar{\varrho}\rangle(t) = \int_0^\infty \frac{dq}{\pi\ell_p}\left\{\frac{1}{q^2+f_<}(e^{-2q^2[q^2t+F(t)]}-1) + 2q^2\int_0^t d\tilde{t}e^{-2q^2[q^2(t-\tilde{t})+F(t)-F(\tilde{t})]}\right\}$$
$$\overset{f_<\to\infty}{=} \int_0^\infty \frac{dq}{\pi\ell_p}2q^2\int_0^t d\tilde{t}e^{-2q^2[q^2(t-\tilde{t})+F(t)-F(\tilde{t})]}$$
$$\overset{!}{\sim} \int_0^\infty \frac{dq}{\pi\ell_p}\frac{1}{q^2+f(t)} = \frac{1}{2l_p}[f(t)]^{-1/2}, \quad \text{for } t\to 0. \tag{B3}$$

This will comprise an *a posteriori* justification of the quasistatic assumption that entered in the derivation of the right-hand side of Eq. (78).

The argument closely follows Appendix A 2. Inserting the force history

$$F(t) = \int_0^t d\hat{t}f(\hat{t}) = Ct^{\alpha+1}, \tag{B4}$$

with

$$\alpha = -2/3 \overset{!}{<} -1/2, \quad C \approx \left(\frac{\hat{\zeta}L^2}{l_p}\right)^{2/3}, \tag{B5}$$

into Eq. (B3) and changing variables $\hat{t}\to xt$ and $q\to qt^{-1/4}$ yields

$$\langle \Delta\bar{\varrho}\rangle(t) = 2t^{1/4}\int_{\Lambda^{-1}t^{1/4}}^\infty \frac{dq}{\pi\ell_p}q^2 \times \int_0^1 dx e^{-2q^2[q^2(1-x)+Ct^{\alpha+1/2}(1-x^{\alpha+1})]}. \tag{B6}$$

As in Appendix A 2 an approximation to the integral can be found in the limit

$$Ct^{\alpha+1/2} \gg 1. \tag{B7}$$

We split the q integral at K satisfying

$$q_\star^{1/3} \gg K \gg q_\star \equiv (Ct^{\alpha+1/2})^{-1/2}, \tag{B8}$$

which can be found in the limit $t\ll 1$ ($\Rightarrow q_\star \ll 1$) because $\alpha < -1/2$. The upper part of the integral

$$\langle \Delta\bar{\varrho}^>\rangle(t) \equiv (\cdots)\int_K^\infty dq(\cdots) \tag{B9}$$

is dominated by values of x close to 1, and we can linearize the exponent in $1-x$,

$$\langle \Delta\bar{\varrho}^>\rangle(t) = 2t^{1/4}\int_K^\infty \frac{dq}{\pi}q^2\int_0^1 dx e^{-2q^2(1-x)[q^2+(\alpha+1)Ct^{\alpha+1/2}]}$$
$$= \tau^{1/4}\int_K^\infty \frac{dq}{\pi}\frac{1-e^{-2q^2(1-x)[q^2+(\alpha+1)Ct^{\alpha+1/2}]}}{q^2+(\alpha+1)Ct^{\alpha+1/2}}$$
$$\sim \tau^{1/4}\int_K^\infty \frac{dq}{\pi}\frac{1}{q^2+(\alpha+1)Ct^{\alpha+1/2}}$$
$$= \frac{1}{l_p\sqrt{(\alpha+1)Ct^\alpha}}\int_{K/\sqrt{(\alpha+1)Ct^{\alpha+1/2}}}^\infty \frac{dq}{1\pi}\frac{1}{q^2+1}$$
$$\sim \frac{1}{2l_p\sqrt{f(t)}}, \tag{B10}$$

where the asymptotics follows from both inequalities in Eqs. (B7) and (B8). The lower part $\langle \Delta\bar{\varrho}^<\rangle$ of the integral is estimated to be subdominant as compared to $\langle \Delta\bar{\varrho}^>\rangle$,

$$\langle \Delta\bar{\varrho}^<\rangle(t) = (\cdots)\int_0^K dq(\cdots) < \frac{2t^{1/4}}{l_p}\int_0^K \frac{dq}{\pi}q^2\int_0^1 dx$$
$$= \frac{t^{1/4}K^3}{3\pi l_p} \ll \frac{C^{-1/2}t^{-\alpha/2}}{3\pi l_p} \propto \langle \Delta\bar{\varrho}^>\rangle(t), \tag{B11}$$

where the first inequality in Eq. (B8) has been applied. Therefore $\langle \Delta\bar{\varrho}\rangle(t)$ is asymptotically given by Eq. (B10).

Finally, we want to emphasize the central condition for the validity of the quasistatic approximation,

$$Ct^{\alpha+1/2} \approx \left(\frac{\hat{\zeta}L^2}{l_p}\right)^{2/3}t^{-1/6} \gg 1, \tag{B12}$$

or $t\ll t_\star$ with $t_\star = (L^2/\ell_p)^4$ as given by Eq. (73).

APPENDIX C: DEFINING $t_\star$

As anticipated in part I, there is a problem-specific time $t_\star$ limiting the short-time validity of OPT. Physically, the crossover at $t_\star$ can be understood as follows. For $t\gg t_\star$ the "speed" of the structural relaxation is determined solely by the relaxation times of the bending modes, which are related to the transverse friction while the longitudinal friction is irrelevant. In contrast, for $t\ll t_\star$ the longitudinal friction substantially limits the speed of the relaxation. This suggests to estimate the time $t_\star$ as follows. From the continuity equation (1), derived via the MSPT, we can estimate the order of magnitude of the correction $\delta f(s,t) = f(s,t) - f^{\mathrm{OPT}}$ to the flat tension profile, Eq. (69), by

$$\delta f \approx \hat{\zeta}\partial_t\langle\Delta\bar{\varrho}\rangle(f^{\mathrm{OPT}},t)L^2. \tag{C1}$$

OPT can only be applicable if the correction δf has negligible effect on the evolution of the stored length,

$$\left|1-\frac{\langle\Delta\bar{\varrho}\rangle(f^{\mathrm{OPT}}+\delta f,t)}{\langle\Delta\bar{\varrho}\rangle(f^{\mathrm{OPT}},t)}\right| \ll 1, \quad \text{for } t \gg t_\star. \tag{C2}$$

The time for which the left-hand side of Eq. (C2) becomes of order unity may thus be identified with the time $t_\star$ before which OPT is not valid.

[1] P. G. de Gennes, *Scaling Concepts in Polymer Physics* (Cornell University Press, Ithaca, 1979).
[2] C. Bustamante, Z. Bryant, and S. B. Smith, Nature (London) **421**, 423 (2003).
[3] P. A. Janmey and D. A. Weitz, Trends Biochem. Sci. **29**, 364 (2004).
[4] Y. Sawada and M. P. Sheetz, J. Cell Biol. **156**, 609 (2002).
[5] G. Forgacs, S. H. Yook, P. A. Janmey, H. Jeong, and C. G. Burd, J. Cell. Sci. **117**, 2769 (2004).
[6] M. Doi and S. F. Edwards, *The Theory of Polymer Dynamics* (Clarendon Press, Oxford, 1986).
[7] O. Hallatschek, E. Frey, and K. Kroy, preceding paper, Phys. Rev. E **75**, 031905 (2007).
[8] B. Obermayer and O. Hallatschek (unpublished).
[9] U. Seifert, W. Wintz, and P. Nelson, Phys. Rev. Lett. **77**, 5389 (1996).
[10] R. Everaers, F. Jülicher, A. Ajdari, and A. C. Maggs, Phys. Rev. Lett. **82**, 3717 (1999).
[11] D. C. Morse, Macromolecules **31**, 7044 (1998).
[12] F. Brochard-Wyart, A. Buguin, and P. G. de Gennes, Europhys. Lett. **47**, 171 (1999).
[13] B. Obermayer, K. Kroy, E. Frey, and O. Hallatschek (unpublished).
[14] R. Granek, J. Phys. II **7**, 1761 (1997).
[15] F. Gittes and F. C. MacKintosh, Phys. Rev. E **58**, R1241 (1998).
[16] C. Bustamante, J. Marko, E. Siggia, and S. Smith, Science **265**, 1599 (1994).
[17] Y. Bohbot-Raviv, W. Z. Zhao, M. Feingold, C. H. Wiggins, and R. Granek, Phys. Rev. Lett. **92**, 098101 (2004).
[18] O. Hallatschek, E. Frey, and K. Kroy, Phys. Rev. Lett. **94**, 077804 (2005).
[19] M. Toda, R. Kubo, and N. Saito, *Statistical Physics I: Equilibrium Statistical Mechanics* (Springer, Berlin, 1983).
[20] R. Kubo, M. Toda, and N. Hashitsume, *Statistical Physics II: Nonequilibrium Statistical Mechanics* (Springer, Berlin, 1992).
[21] P. Ranjith and P. B. Sunil Kumar, Phys. Rev. Lett. **89**, 018302 (2001).
[22] L. Le Goff, F. Amblard, and E. M. Furst, Phys. Rev. Lett. **88**, 018101 (2002).
[23] T. T. Perkins, D. E. Smith, and S. Chu, Science **276**, 2016 (1997).
[24] S. R. Quake, H. Babcock, and S. Chu, Nature (London) **388**, 151 (1997).
[25] L. Le Goff, O. Hallatschek, E. Frey, and F. Amblard, Phys. Rev. Lett. **89**, 258101 (2002).
[26] B. Maier, U. Seifert, and J. Rädler, Europhys. Lett. **60**, 622 (2002).
[27] F. Brochard-Wyart, Europhys. Lett. **23**, 105 (1993).
[28] F. Brochard-Wyart, Europhys. Lett. **30**, 387 (1995).
[29] S. Manneville, P. Cluzel, J.-L. Viovy, D. Chatenay, and F. Caron, Europhys. Lett. **36**, 413 (1996).
[30] B. Obermayer, K. Kroy, E. Frey, and O. Hallatschek (unpublished).
[31] B. Mickey and J. Howard, J. Cell Biol. **130**, 909 (1995).
[32] F. Pampaloni, G. Lattanzi, A. Jonas, T. Surrey, E. Frey, and E.-L. Florin, Proc. Natl. Acad. Sci. U.S.A. **103**, 10248 (2006).
[33] V. Shankar, M. Pasquali, and D. C. Morse, J. Rheol. **46**, 1111 (2002).
[34] M. L. Gardel, M. T. Valentine, J. C. Crocker, A. R. Bausch, and D. A. Weitz, Phys Rev Lett, **91**, 158302 (2003).
[35] B. Obermayer, O. Hallatschek, E. Frey, and K. Kroy, e-print cond-mat/0603556.
[36] T. Munk, O. Hallatschek, C. H. Wiggins, and E. Frey, Phys. Rev. E **74**, 041911 (2006).